AD-A273 806

PL-TR-93-2178

THE PROTEL CONTAMINATION CODE

C. A. Hein

Radex, Inc.
Three Preston Court
Bedford, MA 01730

31 July 1993

Scientific Report No. 4

Approved for public release; distribution unlimited

PHILLIPS LABORATORY
Directorate of Geophysics
AIR FORCE MATERIEL COMMAND
HANSCOM AIR FORCE BASE, MA 01731-3010

"This technical report has been reviewed and is approved for publication"

EDWARD C. ROBINSON
Contract Manager
Data Analysis Division

ROBERT E. McINERNEY, Director
Data Analysis Division

This report has been reviewed by the ESD Public Affairs Office (PA) and is releasable to the National Technical Information Service (NTIS).

Qualified requestors may obtain additional copies from the Defense Technical Information Center. All others should apply to the National Technical Information Service.

If your address has changed, or if you wish to be removed from the mailing list, or if the addressee is no longer employed by your organization, please notify PL/TSI, 29 Randolph Road, Hanscom AFB, MA 01731-3010. This will assist us in maintaining a current mailing list.

Do not return copies of this report unless contractual obligations or notices on a specific document requires that it be returned.

REPORT DOCUMENTATION PAGE

Form Approved
OMB No. 0704-0188

1. AGENCY USE ONLY (*Leave blank*)	2. REPORT DATE	3. REPORT TYPE AND DATES COVERED
	31 July 1993	Scientific Report No. 4

4. TITLE AND SUBTITLE
The PROTEL Contamination Code

5. FUNDING NUMBERS
PE 62101F
PR 7601 TA 22 WU RA
Contract F19628-90-C-0090

6. AUTHOR(S)
C. A. Hein

7. PERFORMING ORGANIZATION NAME(S) AND ADDRESS(ES)
RADEX, Inc.
Three Preston Court
Bedford, MA 01730

8. PERFORMING ORGANIZATION REPORT NUMBER
RXR-93071

9. SPONSORING/MONITORING AGENCY NAME(S) AND ADDRESS(ES)
Phillips Laboratory
29 Randolph Road
Hanscom AFB, MA 01731-3010
Contract Manager: Edward Robinson/GPD

10. SPONSORING/MONITORING AGENCY REPORT NUMBER
PL-TR-93-2178

11. SUPPLEMENTARY NOTES

12a. DISTRIBUTION/AVAILABILITY STATEMENT
Approved for Public Release
Distribution Unlimited

12b. DISTRIBUTION CODE

13. ABSTRACT (*Maximum 200 words*)

The Proton Telescope (PROTEL) was one of several instruments used to measure the proton populations encountered by the Combined Radiation and Release Experimental Satellite (CRRES) in its 15 months of successful operation. In the radiation environment encountered by CRRES, the PROTEL instrument was subjected to "contamination" caused by the penetration of high energy protons passing through the instrument outside its nominal aperture, falsely trigger a valid detection response. The PROTEL contamination code was written to model the performance of the PROTEL High Energy Head (HEH) which is designed to respond to protons in the 10-100 MeV range. This report provides a brief description of the contamination code, the methodology underlying the modeling used, together with a summary of results. Tables and graphs describing the PROTEL contamination response for isotropic and mirror plane proton distributions are provided. The results of the modeling have been sucessfully used to compare PROTEL observations with observations made by the CRRES radiation dosimeter and proton instruments aboard other satellites.

14. SUBJECT TERMS
Proton telescope (PROTEL), CRRES satellite, Isotropic and mirror plane proton distributions, Space radiation environment, Instrument modeling, Monte Carlo computations

15. NUMBER OF PAGES
30

16. PRICE CODE

17. SECURITY CLASSIFICATION OF REPORT	18. SECURITY CLASSIFICATION OF THIS PAGE	19. SECURITY CLASSIFICATION OF ABSTRACT	20. LIMITATION OF ABSTRACT
Unclassified	Unclassified	Unclassified	Unlimited

TABLE OF CONTENTS

List of Figures

List of Tables

ACKNOWLEDGEMENTS

The author would like to thank Bob Redus, Bob Filz, Susan Gussenhoven of P.L. and Jim Bass of Radex, Inc., for many useful and helpful discussions and suggestions concerning the research described in this report.

1. INTRODUCTION

The Proton Telescope (PROTEL) is one of several instruments used to measure proton energy and flux on the CRRES satellite. Multiple proton instruments (of different types) were used to obtain data over a wide energy range, and to provide redundancy where there is an overlap. The PROTEL instrument is a sophisticated proton detector designed to operate in a hostile environment, where it was subjected to a high density flux of electrons, protons and, to a lesser extent, heavier ions, particularly while passing through the radiation (Van Allen) belts. In addition to using passive shielding techniques and magnetic deflection of electrons, it used an array of silicon particle detectors together with an on-board processor, where the latter used coincidence and anti-coincidence in the detector array (detection logic) to reduce false counts. PROTEL has two detectors, the Low Energy Head (LEH) and High Energy Head (HEH), which cover 1-9 and 6-100 MeV ranges respectively.

In order to properly evaluate the performance of PROTEL, it was necessary to model the behavior of the PROTEL in its hostile environment. In order to do so, it is necessary to anticipate deviations of the PROTEL instrument from its nominal design, to identify the potential sources of errors due to limitations of the PROTEL design and due to the hostile environment. In the radiation belts, it was expected that the LEH would be swamped by the high flux environment, but the performance of the HEH would depend upon the proton energy spectrum.

In a report [*Redus, et al.*, 1990] it was found that PROTEL will have problems resulting from the penetration of high energy protons (above 100 MeV) from certain angles outside the entrance cone. These protons will produce false counts (contamination) in the data. The effect of contamination on observed counts will strongly depend upon the energy spectrum and angular distribution of the high energy protons. For this reason, a software package (PROTEL Contamination Code) which models the contamination problem for the HEH was developed.

This report describes the PROTEL Contamination Code, and the results of the contamination modeling obtained from its use. Section 2 provides a brief description of the HEH detector. Section 3 provides a brief description of the methodology used to develop and verify the code. Section 4 provides a summary of the results obtained using the code. The Appendices provide tables and graphs of some of the results of the contamination code computations.

The results provided here indicate that for certain "hard" proton spectra, particularly in the range between 100 and 400 MeV, the PROTEL HEH will subjected to a high level of "contamination". The results obtained from this study (response functions) have been used to compare PROTEL data with data obtained from the CRRES dosimeters, and corrections obtained from the Protel modeling described here for the isotropic case have been successfully applied to the CRRES dosimeter data and to data obtained from other satellite instruments [*Violet*, 1992].

The approach developed here could be useful in developing and evaluating designs of future proton telescopes.

2. BRIEF DESCRIPTION OF THE PROTEL HIGH ENERGY HEAD

A detailed description of the PROTEL instrument is provided in a recent report [*Lynch, et al.*, 1989]. PROTEL collected proton flux data in the 1 to 100 MeV energy range in the radiation belts. It consisted of two detector instruments, the low energy head [LEH] (1 - 10 MeV) and the high energy head [HEH] (6 - 100 MeV) and a dedicated processor which processes the raw data from the detectors, and at 1 second intervals, hands off the reduced data to the satellite's telemetry system. The reduced data consists of counts in 24 energy channels (8 for LEH, 16 for HEH) spaced logarithmically in the 1 - 100 MeV energy interval, together with environmental data and raw counts for the solid state particle detectors.

The PROTEL HEH detector contains six solid state detectors D1-D6. D1-D5 each contain two detection areas, the central disk, and a ring surrounding the disk. D6 has only a circular disk. Pulse height circuitry, coincidence and anti-coincidence circuitry and logic are used to classify detection events in the several particle detectors. A detection event is recorded in one of the energy channels only if it meets the energy deposit requirements of the detectors associated with the energy channel and the requirements of the coincidence/anticoincidence logic. The ring detectors and D6 are used in connection with the anti-coincidence logic. The anti-coincidence logic is used to reduce or eliminate counts due to protons which enter through the back or enter the detector from directions outside the nominal acceptance cone.

3. DESCRIPTION OF THE PROTEL CONTAMINATION CODE

The assumptions made in developing the PROTEL contamination code are as follows:

The primary effect is due to protons which penetrate the PROTEL housing/shielding and are decelerated in the direction of motion while interacting with the electrons in the material through which they pass. The protons are assumed to travel in straight lines until they either are stopped by or penetrate the material they are passing through. This is a relatively good assumption for high energy protons. However, important effects are neglected, such as Coulomb scattering with the nuclei, inelastic scattering off of the nuclei, including "STARS" -- nuclear reactions which produce protons, neutrons and/or gamma rays.

Under this assumption, the computation of contamination effects proceeds as follows:

(1) A simplified mathematical description of the mass/geometry of the HEH was developed using the original blueprints. From the latter, measurements were made of the different materials used in the construction of the HEH and their locations. The materials used were aluminum, iron, brass and tungsten. In addition, a magnet was used to deflect high energy electrons. The magnet was made of samarium and cobalt. From the blueprint diagrams of the magnet, it was not possible to determine the location of the actual boundary between the iron magnet holder and the magnet pieces. Partly, for this reason, and partly to simplify the computations, it was decided to treat the entire magnet as iron.

(2) A ray tracing algorithm was developed which would determine the number of layers, compute the thickness of each layer and identify the materials which a ray pointing in an arbitrary direction (starting from an arbitrary point within the detector volume) would encounter. Except for the case in which the path intersects the ridges on the inside surface of the PROTEL HEH baffle, the computed thicknesses are

accurate to approximately 0.1 mm which is better than the estimated 0.5 mm accuracy to which the dimensions of the various components of the PROTEL housing/shielding can be measured from the blueprints. Using the Janni energy-range relations and the Janni tables [*Janni*, 1982] a fast algorithm was developed which would, given a proton input spectrum, compute the spectrum resulting from passage through the materials associated with a given point and direction.

As a test of the methodology, calibration tests of the PROTEL HEH performed at the Harvard University cyclotron were successfully modeled using an early version of the Protel Contamination Code [*Hein*, 1990].

(3) A Monte Carlo code was use to model the behavior of the High Energy Head. For each Monte Carlo trial, a point on the surface of the first detector was randomly selected. Then a direction (unit vector) was randomly selected (based upon the proton pitch angle distribution - isotropic, mirror plane, or $\sin^N \alpha$). For each such point and direction, the ray-tracing routine was used to compute the thickness of each of the material "layers" through which a proton passes in the body and shielding of PROTEL in its path to each reference point on the first detector.

(4) The ray-tracing algorithm has a high computation overhead. For this reason, and the fact that the contamination computation will be repeated for various input spectrum and values of input parameters, it was necessary to generate a file containing the ray trace output data for each of the Monte Carlo "trials". The number N of "trials" required was determined by comparing runs performed with different "seeds"; N = 20,000 points was chosen over a solid angle defined by a 60 degree half-angle. For larger half angles, the fraction of protons which would strike more than one detector was small. The file contains the following information for each of the 20,000 reference points and reference directions:

- (a) The location of the reference point on the first detector.
- (b) The unit vector describing the direction of the ray.
- (c) The number of "layers" of material the ray passes through
- (d) For each layer, a matter flag which indicates what material the ray passes through (aluminum, iron, brass, tungsten, etc.)
- (e) The thickness of each layer.

(6) Because a variety of input spectra would be studied, the *response function* which describes the instrument's response to a flat energy spectrum as a function of energy was computed. For incident energies in the range of 5-105 MeV, the response function was computed at energy intervals of 0.1 MeV; from 105-400 MeV at 1 MeV intervals. The direction and thickness information in the file described above is used to compute the energy loss in each of the material layers using the Janni energy/range relation for each of the materials. For each trial in which the particle actually reaches the first detector, a determination is made, as to which detectors the ray passes through; then the path length through the detector is calculated, and the detector coincidence logic is used to determine the channel into which the corresponding "count" is to be recorded. For each of the incident energies the fraction of counts detected are compared to the total number of trials.

(7) The tabulated response function is then used to compute the actual number of predicted counts for an arbitrary energy spectrum.

4. RESULTS

In Appendix A, Tables A-1 to A-3 give the fraction of PROTEL HEH counts due to contamination for proton energy spectra of the form E^q where E is in MeV and q varies in 0.5 steps from 0 to -6 for an isotropic distribution. Table A-1 gives the contamination due to protons of all energies. Tables A-2 and A-3 give the fraction of the PROTEL HEH counts due to contamination from protons above 100 and 200 MeV respectively. Tables A-4 and A-5 provide the data which corresponds to the first data set of Table A-1 for the mirror plane case, for an orientation of the mirror plane of 0 and 90 degrees with respect to the direction of the maximum obstruction of the electron deflection magnet.

The tables are obtained from integrating the product of the computed response function with the indicated power law spectrum over the total energy range for Tables A-1, A-4, and A-5, and over the ranges $E > 100$ MeV and $E > 200$ MeV for Tables A-2 and A-3. The differences in the entries in Tables A-1 and A-2 reflect the contamination contribution for the range $0 < E < 100$; similarly for Tables A-1 and A-3 ($0 < E < 200$) and Tables A-2 and A-3 ($100 < E < 200$).

In Appendix B the response functions for each of the HEH channels are provided in graphical form in Figures B-1 through B-16 for the isotropic case and Figures B-17 through B-32 for the two mirror plane orientations. For the latter, the two response functions are provided in each graph. The non-contamination response of each detector is represented by a "spike" in the $0 < E < 100$ MeV range, with the spike "width" being the actual channel width. The bulk of the contamination occurs in the $E > 100$ range, as is evident in the graphs. On Figures B-17 through B-32 the two response functions are distinguished by the use of different line types, a solid line and a dashed line for 0 and 90 degrees with respect to the maximum deflection of the electron deflection magnet. The mirror planes are parallel to the HEH body axis; except for the deflection magnet, the HEH housing is cylindrically symmetric with respect to the body axis.

The response function for the isotropic case was used to cross calibrate PROTEL data with data obtained from the CRRES dosimeters and other instruments. The data, associated with solar proton events covered 20 orbits in March and June of 1991. The data was collected at high altitudes and was known to be near-isotropic; the energy spectra appeared to be relatively flat and stable over periods of several hours. This study [*Violet*, 1993] also compared the same PROTEL data with data obtained from the GEOS satellite. In this study, the PROTEL data was fitted to a power law spectrum of the form $(J(10\ \text{Mev})/J(E))^N$. The response function was used to compute corrected values of J(10) and N. The latter were compared, with good agreement to similar fits of data obtained from the CRRES dosimeter and the GEOS detectors. The corrections were found to be substantial, and increase for power law spectra as N approaches 0.

REFERENCES

Hein, C., "Comparison of the PROTEL Contamination Code Predictions with the Harvard Accelerator Calibration Data", GL Technical Memorandum No. 179, 1990

Janni, J., "Proton Range Energy Tables, 1 KeV - 10 GeV" in: Atomic Data and Nuclear Data Tables, Volume 27, 147-529 (1982), Academic Press, New York

Lynch, K., Boughan, E., Fischi, D., Hardy, D., Riehl, K., "PROTEL: Design, Fabrication, Calibration, Testing and Satellite Integration of a Proton Telescope", AFGL-TR-89-0045, Environmental Papers, # 337, 1989, ADA214564.

Redus, R., Filz, R., Swider, W., Violet, M., "Protel Analysis Report", 1990 (draft).

Violet, M. D., Lynch, K., Redus, R., Riehl, K., Boughan, E., Hein, C. "The Proton Telescope (PROTEL) on the CRRES Spacecraft", IEEE Transactions on Nuclear Science, v. 40, p. 242, 1993.

Violet, M. "Understanding Protel", Private Communication 1992 (draft report in progress)

APPENDIX A.

Table A-1
FRACTION OF PROTEL HEH COUNTS DUE TO CONTAMINATION
Isotropic Distribution
POWER LAW SPECTRUM E**q

CHAN	q = 0	-.5	-1.0	-1.5	-2.0	-2.5	-3.0	-3.5	-4.0	-4.5	-5.0	-5.5	-6.0
1	.9928	.9606	.8153	.4671	.1882	.0950	.0687	.0581	.0513	.0460	.0416	.0377	.0343
2	.9833	.9210	.7056	.3537	.1421	.0739	.0526	.0433	.0373	.0327	.0289	.0255	.0227
3	.9659	.8616	.6045	.3344	.2086	.1660	.1491	.1396	.1326	.1268	.1217	.1171	.1129
4	.9642	.8607	.5986	.2906	.1293	.0729	.0526	.0430	.0371	.0326	.0290	.0260	.0234
5	.9768	.9152	.7416	.4557	.2313	.1313	.0943	.0791	.0712	.0662	.0626	.0599	.0579
6	.9736	.9119	.7556	.5167	.3267	.2338	.1949	.1767	.1660	.1584	.1522	.1468	.1421
7	.9721	.9103	.7543	.5002	.2746	.1539	.1018	.0786	.0663	.0583	.0523	.0475	.0434
8	.9817	.9459	.8535	.6673	.4246	.2340	.1314	.0839	.0613	.0489	.0412	.0356	.0314
9	.9762	.9370	.8474	.6868	.4882	.3256	.2274	.1753	.1472	.1304	.1190	.1104	.1034
10	.9828	.9573	.8993	.7846	.6071	.4114	.2582	.1643	.1125	.0837	.0666	.0553	.0471
11	.9739	.9406	.8733	.7573	.5996	.4388	.3129	.2303	.1800	.1492	.1292	.1153	.1048
12	.9835	.9643	.9255	.8537	.7379	.5855	.4283	.2995	.2101	.1532	.1175	.0944	.0786
13	.9770	.9543	.9127	.8430	.7403	.6128	.4818	.3689	.2837	.2241	.1835	.1554	.1353
14	.9852	.9717	.9473	.9052	.8381	.7423	.6240	.5000	.3888	.3008	.2366	.1914	.1596
15	.9872	.9770	.9594	.9299	.8830	.8137	.7207	.6102	.4952	.3897	.3028	.2362	.1874
16	.9884	.9807	.9682	.9485	.9182	.8735	.8113	.7306	.6346	.5310	.4297	.3391	.2636

Table A-2
FRACTION OF PROTEL HEH COUNTS DUE TO CONTAMINATION
due to protons with E > 100 MeV
Isotropic Distribution
POWER LAW SPECTRUM E**q

CHAN	q = 0	-.5	-1.0	-1.5	-2.0	-2.5	-3.0	-3.5	-4.0	-4.5	-5.0	-5.5	-6.0
1	.9893	.9503	78[illegible]	.4031	.1104	.0224	.0042	.0008	.0001	.0000	.0000	.0000	.0000
2	.9765	.9039	.6[illegible]	.2909	.0775	.0169	.0035	.0007	.0002	.0000	.0000	.0000	.0000
3	.9458	.8088	.4919	.1783	.0462	.0107	.0025	.0006	.0001	.0000	.0000	.0000	.0000
4	.9494	.8282	.5395	.2178	.0617	.0153	.0037	.0009	.0002	.0001	.0000	.0000	.0000
5	.9650	.8887	.6867	.3699	.1348	.0396	.0109	.0029	.0008	.0002	.0001	.0000	.0000
6	.9546	.8674	.6615	.3638	.1426	.0462	.0140	.0042	.0013	.0004	.0001	.0000	.0000
7	.9570	.8794	.6960	.4132	.1769	.0615	.0197	.0062	.0019	.0006	.0002	.0001	.0000
8	.9718	.9265	.8169	.6072	.3463	.1532	.0582	.0207	.0073	.0025	.0009	.0003	.0001
9	.9595	.9041	.7859	.5855	.3513	.1721	.0742	.0302	.0121	.0048	.0020	.0008	.0003
10	.9727	.9388	.8662	.7299	.5286	.3171	.1615	.0742	.0325	.0140	.0060	.0026	.0011
11	.9563	.9087	.8184	.6707	.4800	.2961	.1620	.0823	.0404	.0197	.0096	.0047	.0023
12	.9735	.9470	.8962	.8064	.6676	.4925	.3202	.1870	.1017	.0533	.0275	.0142	.0073
13	.9626	.9300	.8730	.7814	.6518	.4972	.3454	.2217	.1347	.0794	.0462	.0268	.0157
14	.9770	.9581	.9249	.8695	.7840	.6657	.5242	.3810	.2580	.1659	.1034	.0635	.0389
15	.9823	.9691	.9467	.9101	.8531	.7706	.6621	.5360	.4079	.2939	.2032	.1370	.0913
16	.9884	.9806	.9682	.9485	.9182	.8735	.8112	.7304	.6344	.5308	.4295	.3387	.2631

Table A-3
FRACTION OF PROTEL HEH COUNTS DUE TO CONTAMINATION
due to protons with E > 200 MeV
Isotropic Distribution
POWER LAW SPECTRUM E**q

CHAN	q = 0	-.5	-1.0	-1.5	-2.0	-2.5	-3.0	-3.5	-4.0	-4.5	-5.0	-5.5	-6.0
1	.3742	.3256	.2417	.1105	.0267	.0047	.0008	.0001	.0000	.0000	.0000	.0000	.0000
2	.3436	.2897	.1931	.0759	.0181	.0035	.0006	.0001	.0000	.0000	.0000	.0000	.0000
3	.4039	.3141	.1724	.0559	.0129	.0026	.0005	.0001	.0000	.0000	.0000	.0000	.0000
4	.4096	.3271	.1938	.0706	.0179	.0040	.0008	.0002	.0000	.0000	.0000	.0000	.0000
5	.4049	.3421	.2412	.1178	.0386	.0102	.0025	.0006	.0001	.0000	.0000	.0000	.0000
6	.4076	.3382	.2339	.1158	.0405	.0116	.0031	.0008	.0002	.0001	.0000	.0000	.0000
7	.4225	.3561	.2569	.1381	.0531	.0165	.0047	.0013	.0003	.0001	.0000	.0000	.0000
8	.4673	.4155	.3400	.2332	.1221	.0492	.0169	.0054	.0017	.0005	.0002	.0000	.0000
9	.4590	.3980	.3163	.2139	.1156	.0506	.0193	.0069	.0024	.0008	.0003	.0001	.0000
10	.5276	.4797	.4152	.3266	.2196	.1215	.0566	.0236	.0093	.0036	.0014	.0005	.0002
11	.5568	.4910	.4070	.3043	.1967	.1085	.0525	.0233	.0099	.0041	.0017	.0007	.0003
12	.7133	.6662	.6023	.5148	.4023	.2781	.1680	.0903	.0448	.0211	.0097	.0044	.0020
13	.7408	.6830	.6075	.5111	.3972	.2794	.1771	.1025	.0555	.0287	.0145	.0072	.0036
14	.8093	.7683	.7144	.6432	.5515	.4418	.3253	.2189	.1356	.0788	.0438	.0237	.0125
15	.8470	.8136	.7703	.7138	.6409	.5504	.4458	.3369	.2366	.1553	.0965	.0576	.0334
16	.9013	.8766	.8447	.8033	.7499	.6826	.6006	.5063	.4060	.3085	.2224	.1531	.1014

Table A-4

FRACTION OF PROTEL NEH COUNTS DUE TO CONTAMINATION
MIRROR PLANE LIMIT, Azimuth = 0 degrees
POWER LAW SPECTRUM E**q

CHAN	q = 0	-.5	-1.0	-1.5	-2.0	-2.5	-3.0	-3.5	-4.0	-4.5	-5.0	-5.5	-6.0
1	.9867	.9245	.6768	.2874	.1022	.0560	.0436	.0382	.0345	.0316	.0290	.0268	.0247
2	.9608	.8377	.5352	.2252	.0872	.0446	.0308	.0248	.0213	.0187	.0166	.0148	.0133
3	.8197	.5192	.2596	.1544	.1196	.1057	.0980	.0928	.0887	.0853	.0823	.0796	.0772
4	.8146	.5089	.2194	.0897	.0458	.0296	.0219	.0174	.0143	.0121	.0104	.0091	.0080
5	.9201	.7522	.4642	.2273	.1186	.0784	.0627	.0554	.0513	.0488	.0472	.0462	.0457
6	.8602	.6428	.3864	.2287	.1605	.1315	.1170	.1082	.1019	.0969	.0929	.0895	.0864
7	.8407	.6098	.3433	.1765	.1016	.0689	.0525	.0427	.0360	.0310	.0271	.0239	.0213
8	.9108	.7695	.5369	.30[illegible]	.1710	.1044	.0733	.0571	.0475	.0410	.0363	.0328	.0301
9	.8697	.7089	.4962	.3184	.2120	.1561	.1258	.1075	.0950	.0857	.0782	.0721	.0668
10	.8986	.7751	.5865	.3897	.2456	.1608	.1141	.0873	.0705	.0588	.0500	.0431	.0374
11	.8696	.7394	.5655	.3990	.2781	.2029	.1579	.1299	.1112	.0977	.0872	.0789	.0719
12	.9030	.8057	.6589	.4897	.3417	.2368	.1704	.1293	.1030	.0851	.0721	.0621	.0542
13	.8904	.7981	.6692	.5256	.3973	.3005	.2341	.1897	.1596	.1382	.1223	.1099	.0999
14	.9153	.8453	.7410	.6107	.4771	.3628	.2769	.2168	.1756	.1469	.1261	.1105	.0983
15	.9239	.8668	.7814	.6696	.5445	.4252	.3260	.2508	.1966	.1582	.1306	.1104	.0951
16	.9288	.8841	.8190	.7321	.6278	.5167	.4113	.3207	.2482	.1929	.1517	.1211	.0982

Table A-5

FRACTION OF PROTEL NEH COUNTS DUE TO CONTAMINATION
MIRROR PLANE LIMIT, Azimuth = 90 degrees
POWER LAW SPECTRUM E**q

CHAN	q = 0	-.5	-1.0	-1.5	-2.0	-2.5	-3.0	-3.5	-4.0	-4.5	-5.0	-5.5	-6.0
1	.9879	.9311	.6980	.3099	.1144	.0635	.0489	.0420	.0374	.0336	.0305	.0278	.0254
2	.9647	.8519	.5629	.2481	.1008	.0537	.0376	.0303	.0257	.0222	.0194	.0171	.0151
3	.8290	.5357	.2747	.1665	.1298	.1144	.1054	.0990	.0938	.0895	.0857	.0823	.0792
4	.8300	.5357	.2426	.1069	.0599	.0419	.0328	.0270	.0228	.0195	.0168	.0146	.0127
5	.9246	.7632	.4806	.2432	.1327	.0912	.0745	.0662	.0612	.0577	.0552	.0534	.0522
6	.8640	.6519	.3994	.2423	.1735	.1439	.1287	.1192	.1122	.1066	.1018	.0977	.0940
7	.8563	.6385	.3729	.1993	.1199	.0852	.0678	.0574	.0500	.0444	.0399	.0361	.0328
8	.9172	.7832	.5545	.3218	.1756	.1052	.0727	.0563	.0469	.0406	.0362	.0330	.0305
9	.8807	.7291	.5208	.3395	.2282	.1693	.1375	.1186	.1059	.0965	.0890	.0829	.0776
10	.9069	.7906	.6065	.4059	.2536	.1625	.1124	.0840	.0666	.0548	.0461	.0394	.0341
11	.8806	.7573	.5866	.4168	.2900	.2100	.1620	.1324	.1129	.0989	.0884	.0800	.0731
12	.9118	.8212	.6804	.5121	.3594	.2485	.1772	.1329	.1046	.0855	.0717	.0613	.0531
13	.8981	.8103	.6849	.5412	.4094	.3080	.2374	.1900	.1578	.1350	.1181	.1051	.0947
14	.9228	.8578	.7589	.6320	.4980	.3803	.2901	.2261	.1819	.1511	.1288	.1121	.0990
15	.9314	.8791	.7995	.6928	.5703	.4503	.3481	.2692	.2117	.1705	.1409	.1190	.1023
16	.9357	.8947	.8341	.7518	.6510	.5410	.4343	.3407	.2648	.2064	.1625	.1298	.1052

APPENDIX B.

This appendix contains graphs of the response functions for the isotropic distribution case (B-1 through B-16) and for two orientations of the Mirror Plane distribution case (B-17 through B-32). For the isotropic case, the response function Monte Carlo computation is based upon 20,000 particles which randomly strike the first detector after passage through the external housing (passive shielding) of the HEH from directions within a cone (for the isotropic distribution) subtending an angle of 60 degrees as measured from the PROTEL HEH axis. The solid angle subtended is π sterradians. The Mirror Plane case is identical, except for the geometry. In this case 20,000 protons are incident on the first detector for incident angles of up to 60 degrees (measured in each mirror plane from the first detector normal) for the two orientations relative to the electron deflection magnet. Note that the Mirror Plane case is more strongly peaked about the nominal entrance cone, as expressed by the channel counts in the 5-100 MeV range.

The number of protons which strike both the first detector and any additional detectors from larger angles will be very small. For this reason the effect of contamination on Channels 1 and 2 will be underestimated, because coincidences are not required for those channels.

Note that the Channels 1 - 16 of the HEH actually correspond to Channels 9 - 24 of the PROTEL instrument.

Note that in the energy interval 5 - 105 MeV, the response function is evaluated at 0.1 MeV intervals; in the interval 105 - 350 MeV, it is evaluated at 1.0 MeV intervals.

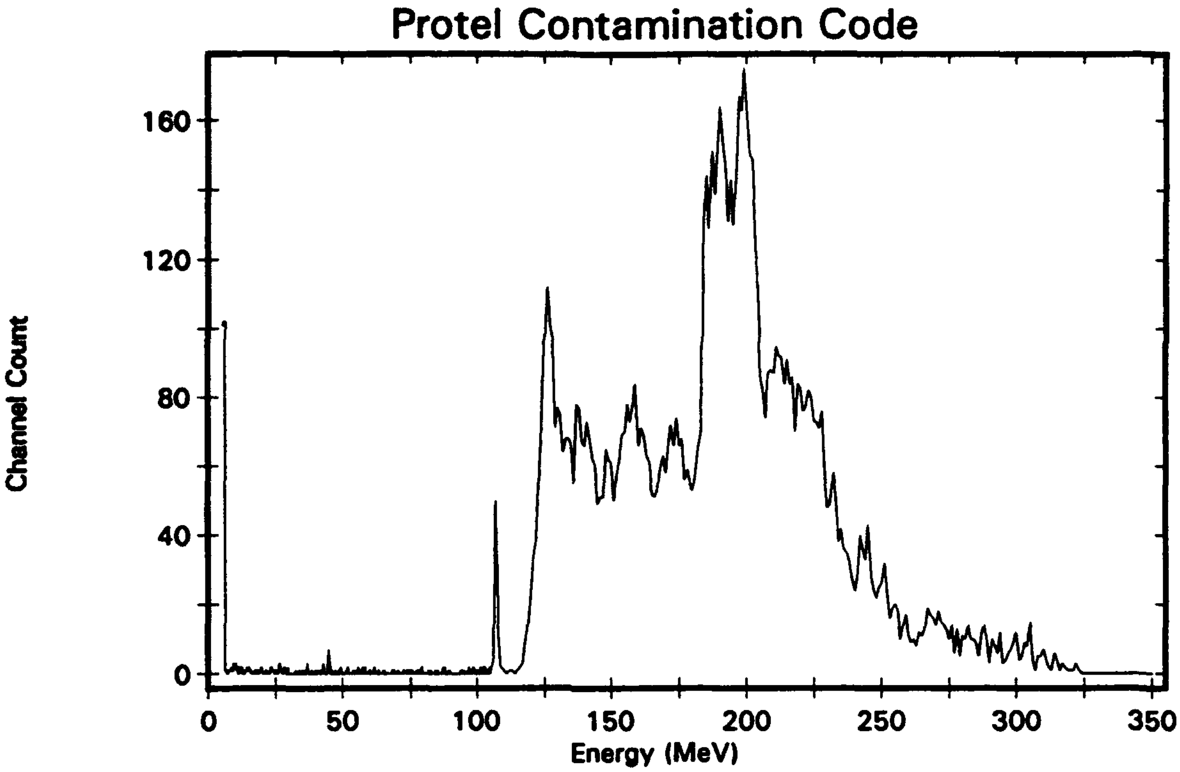

Figure B-1. Isotropic Distribution, Channel 1

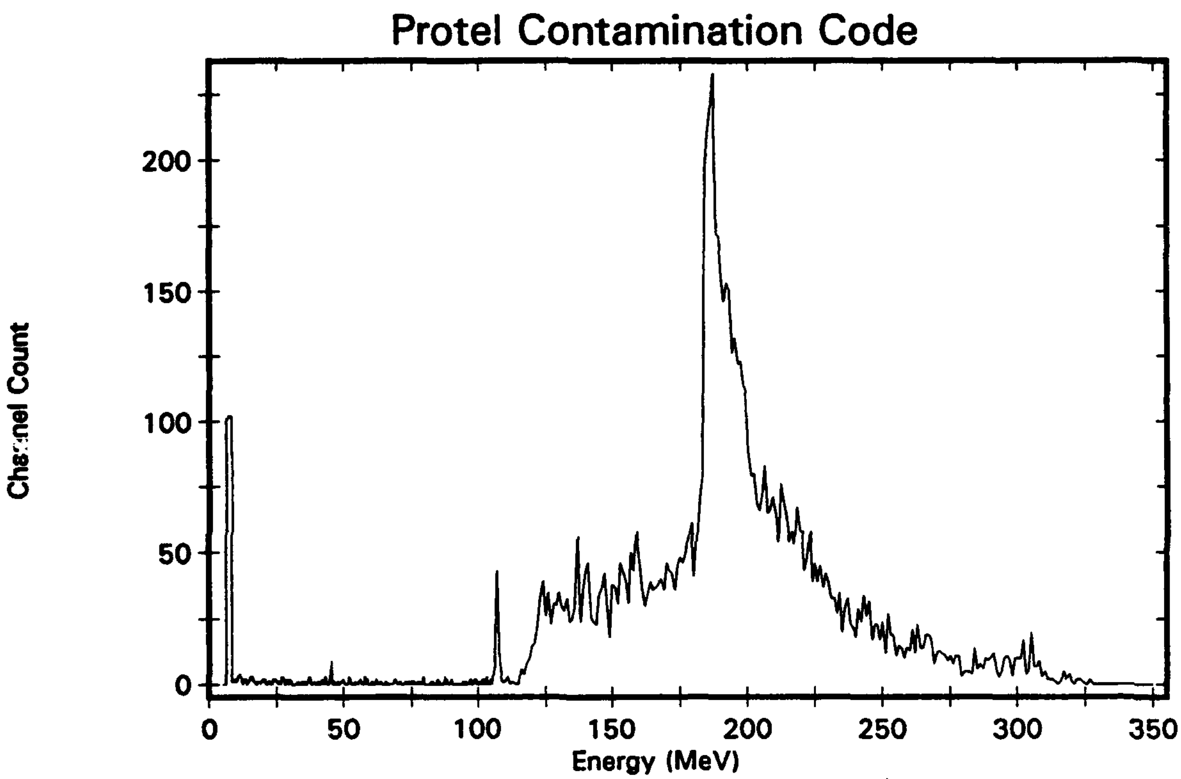

Figure B-2. Isotropic Distribution, Channel 2

DATE RUN: 8/17/93

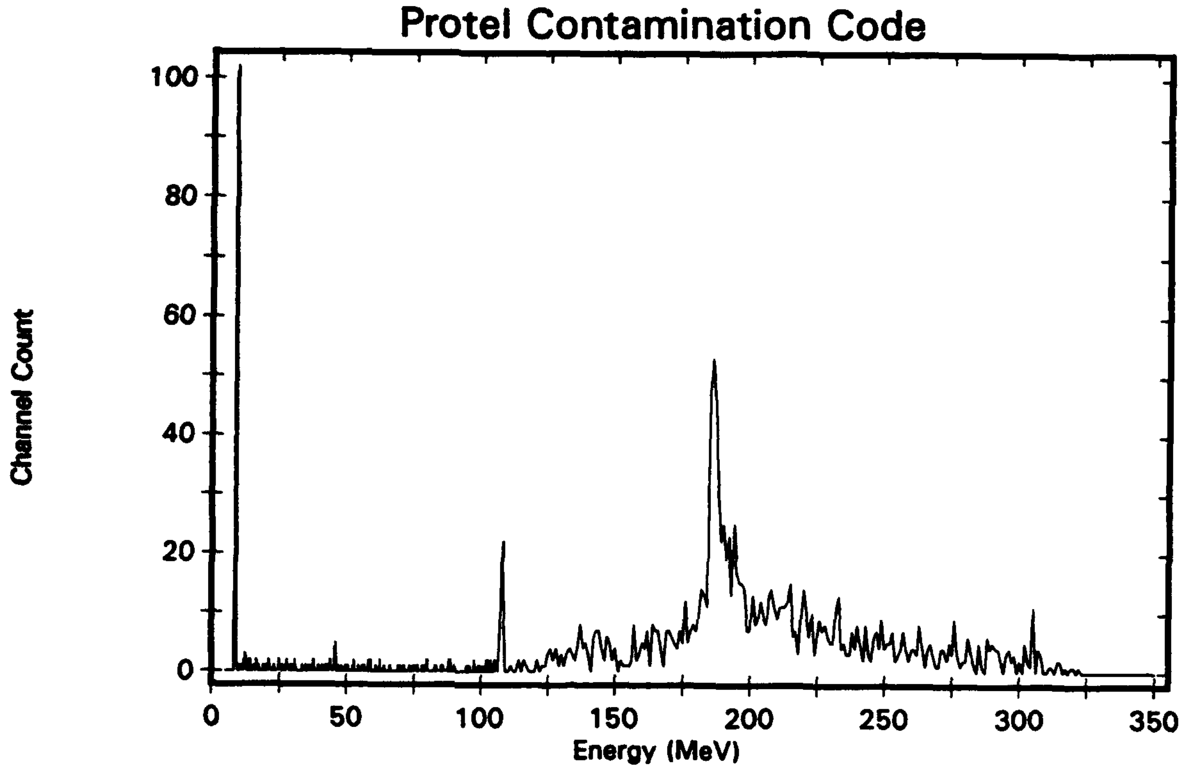

Figure B-3. Isotropic Distribution, Channel 3

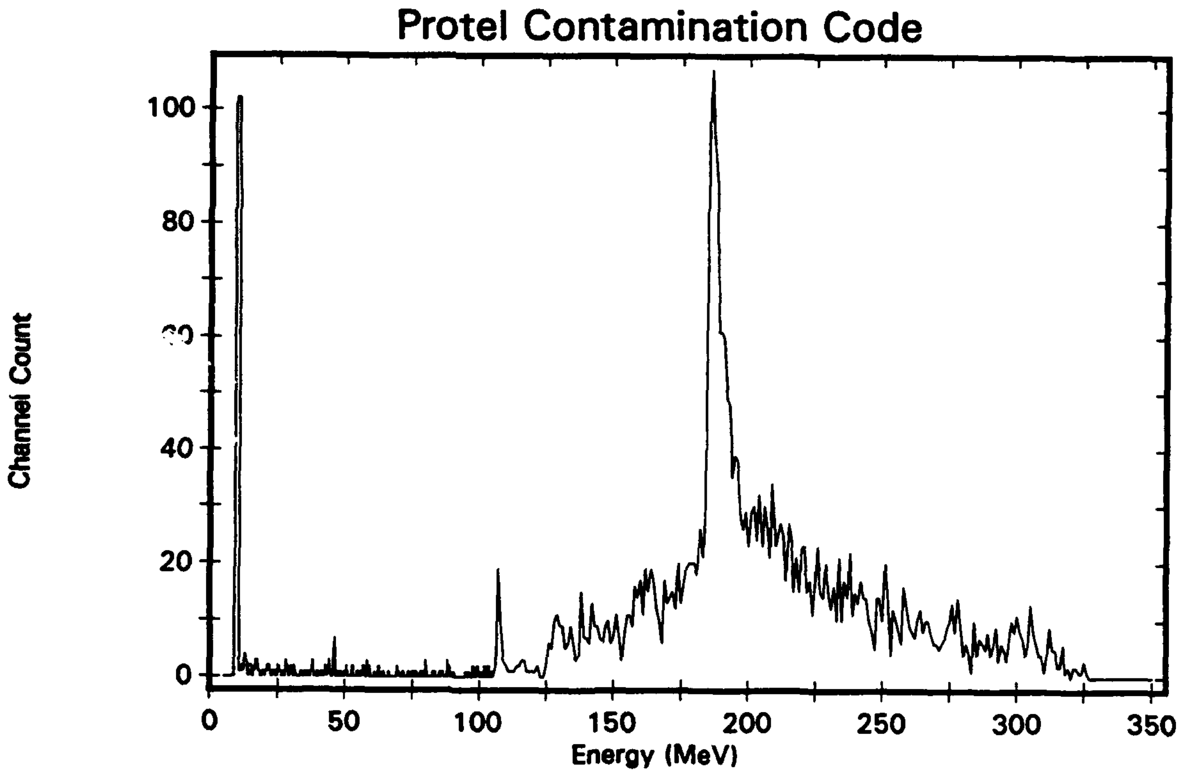

Figure B-4. Isotropic Distribution, Channel 4

DATE RUN: 8/17/93

Protel Contamination Code

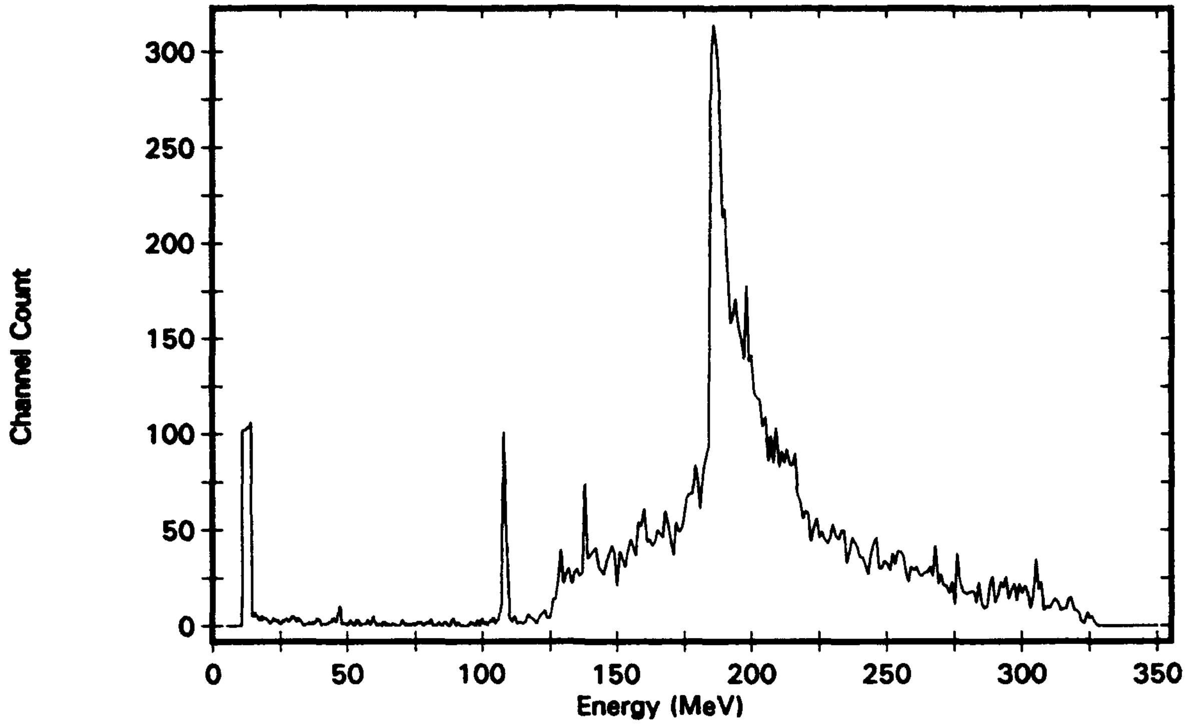

Figure B-5. Isotropic Distribution, Channel 5

Protel Contamination Code

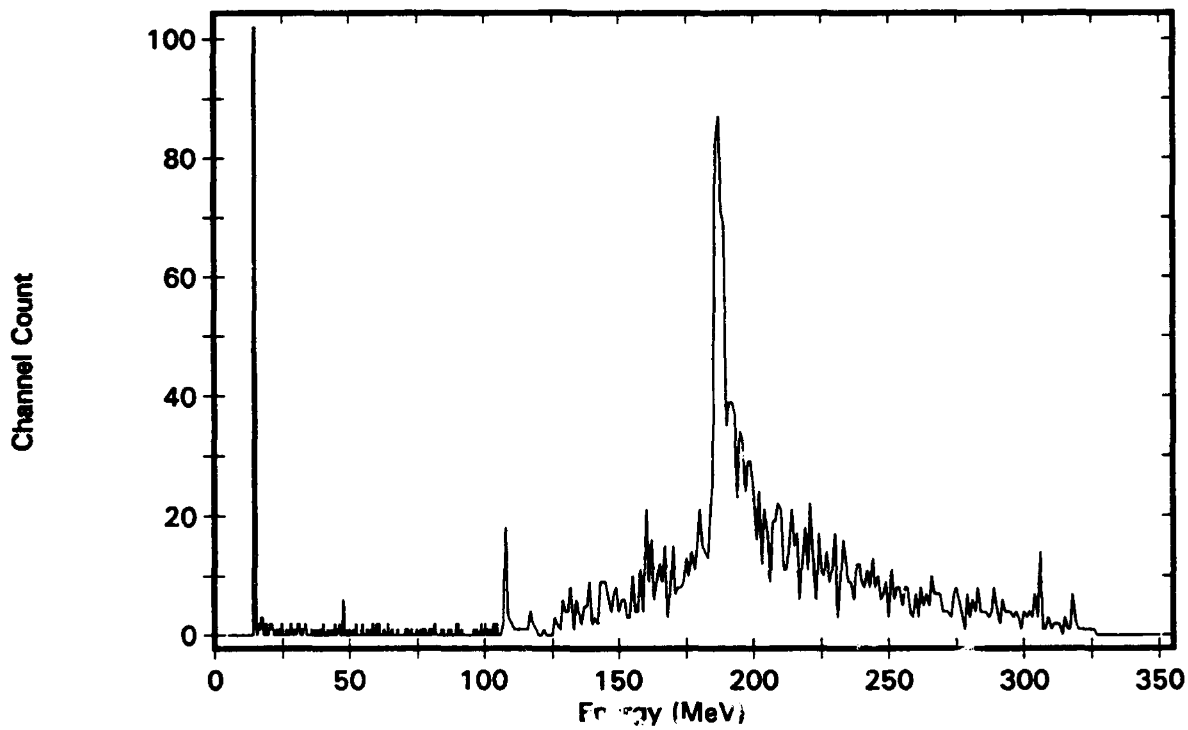

Figure B-6. Isotropic Distribution, Channel 6

DATE RUN: 8/17/93

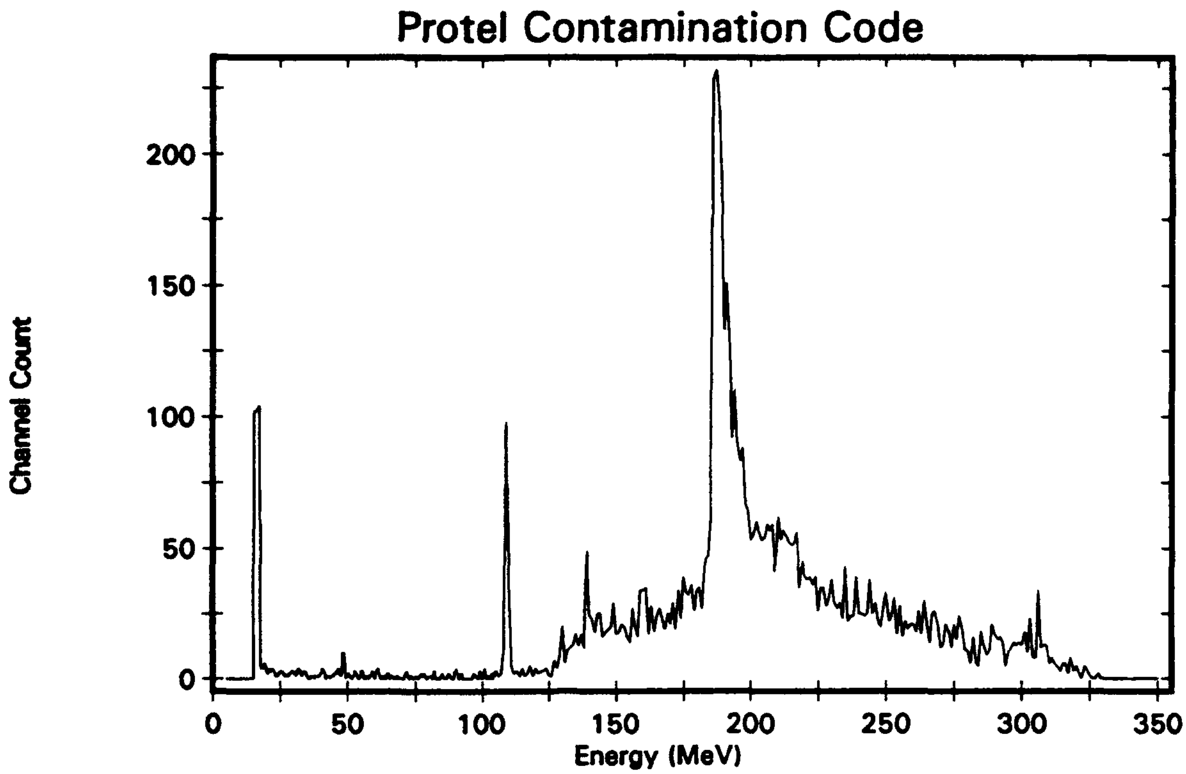

Figure B-7. Isotropic Distribution, Channel 7

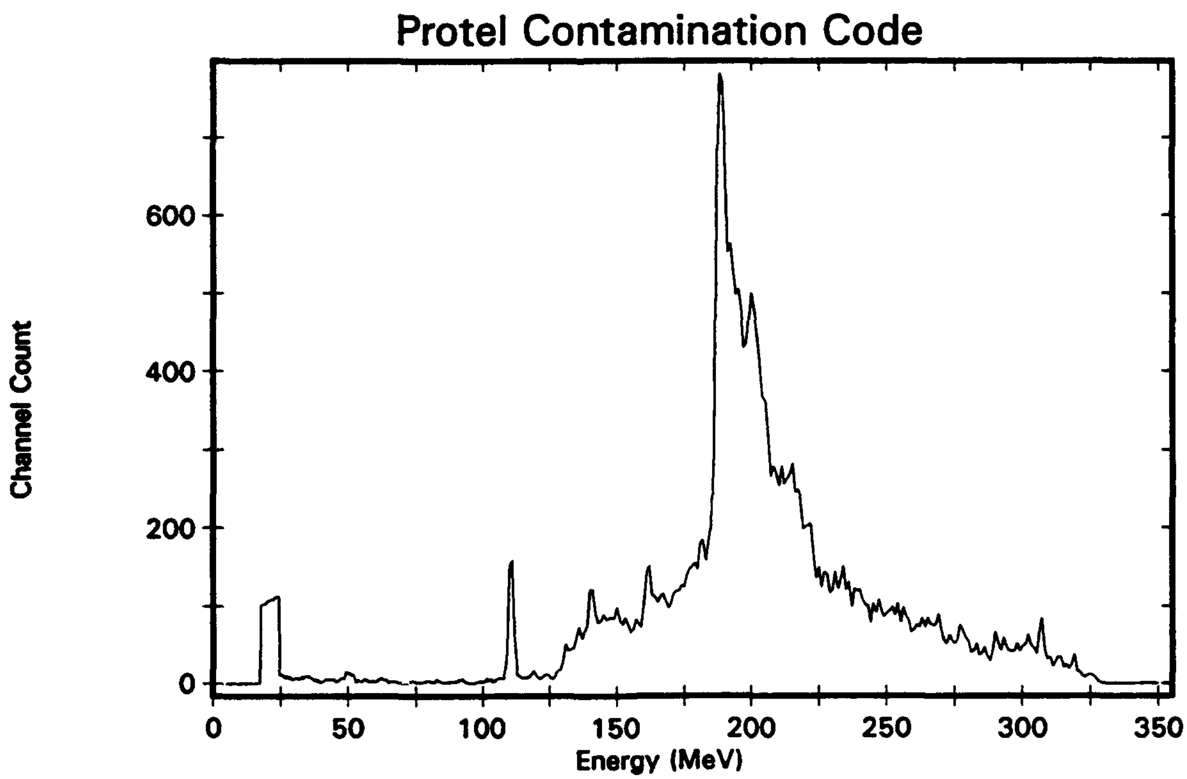

Figure B-8. Isotropic Distribution, Channel 8

DATE RUN: 8/17/93

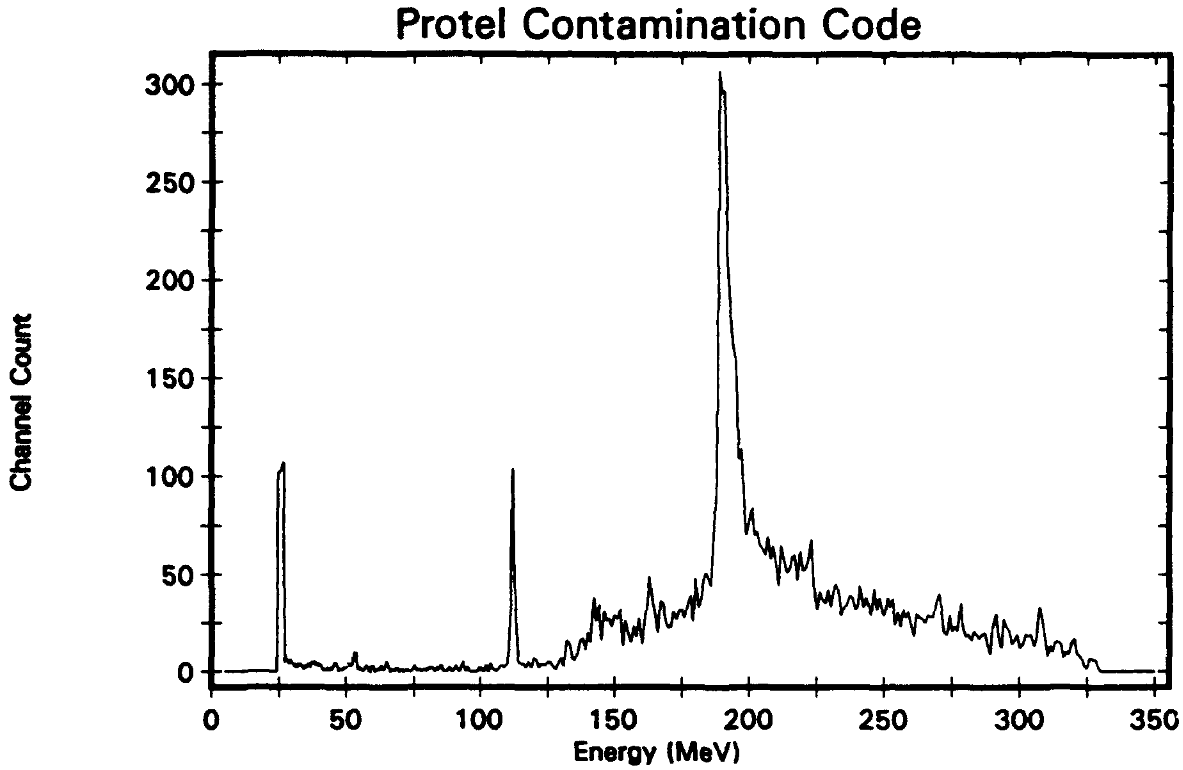

Figure B-9. Isotropic Distribution, Channel 9

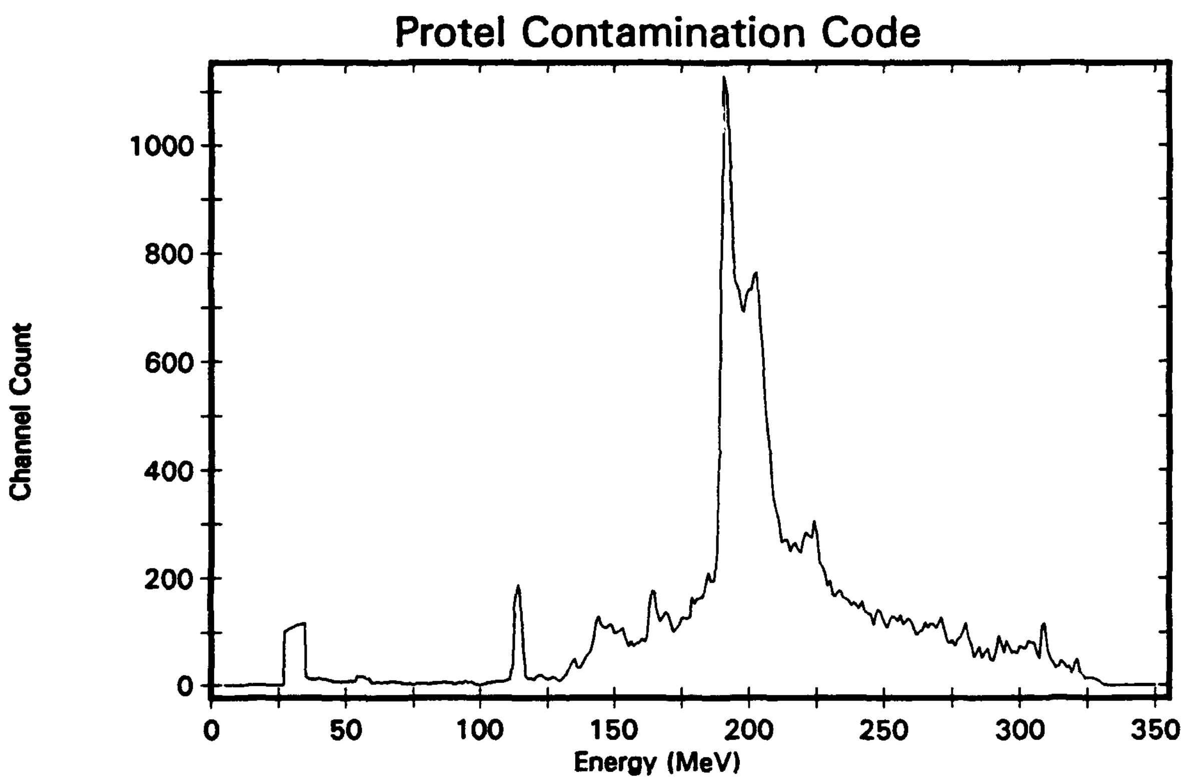

Figure B-10. Isotropic Distribution, Channel 10

DATE RUN: 8/17/93

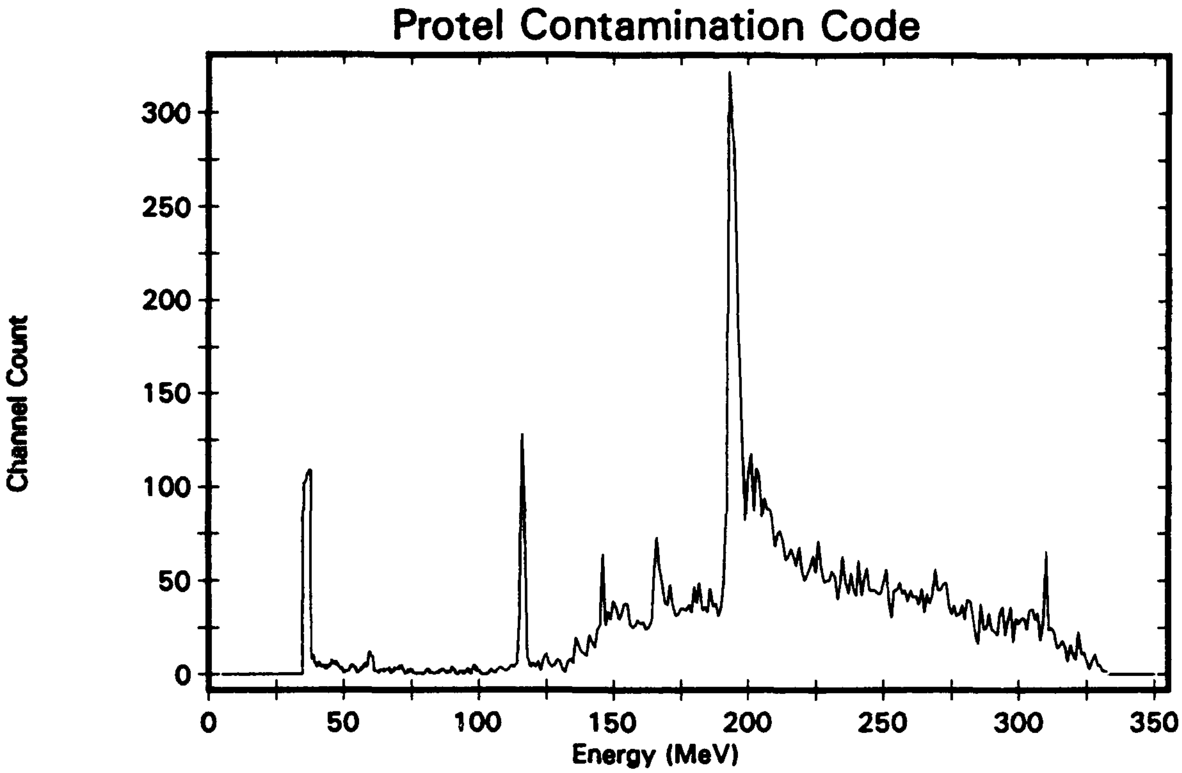

Figure B-11. Isotropic Distribution, Channel 11

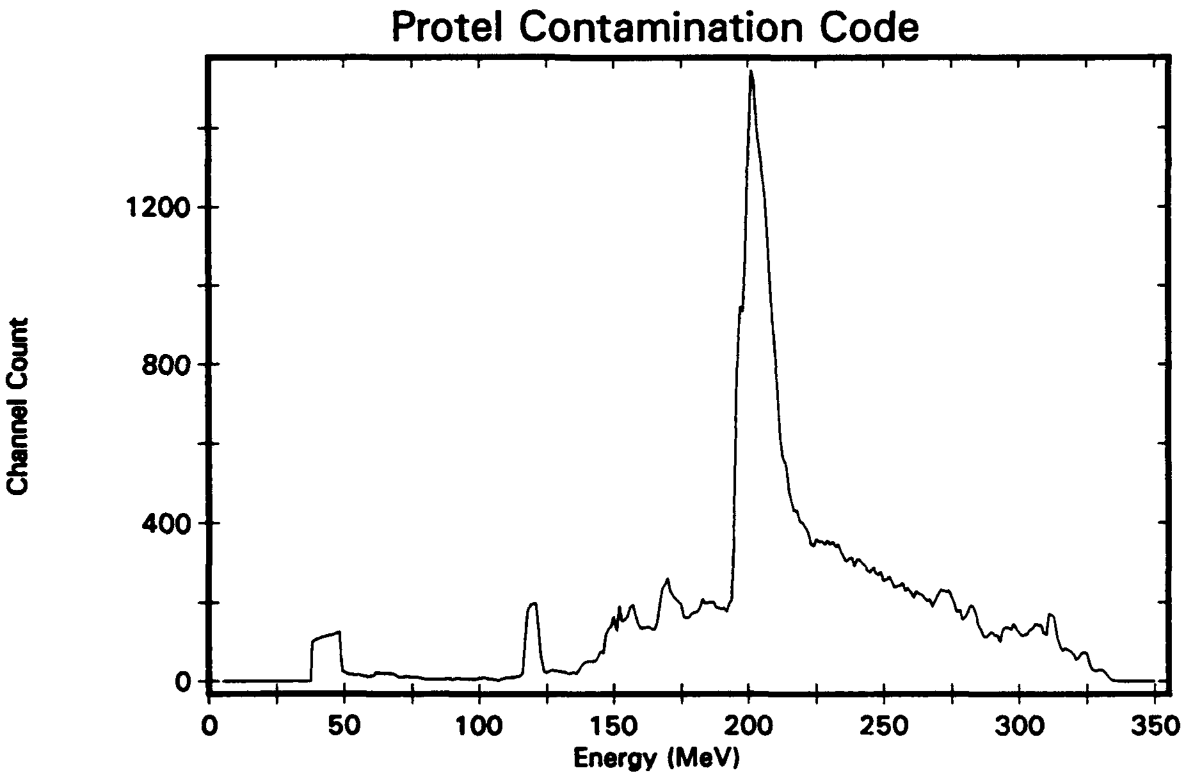

Figure B-12. Isotropic Distribution, Channel 12

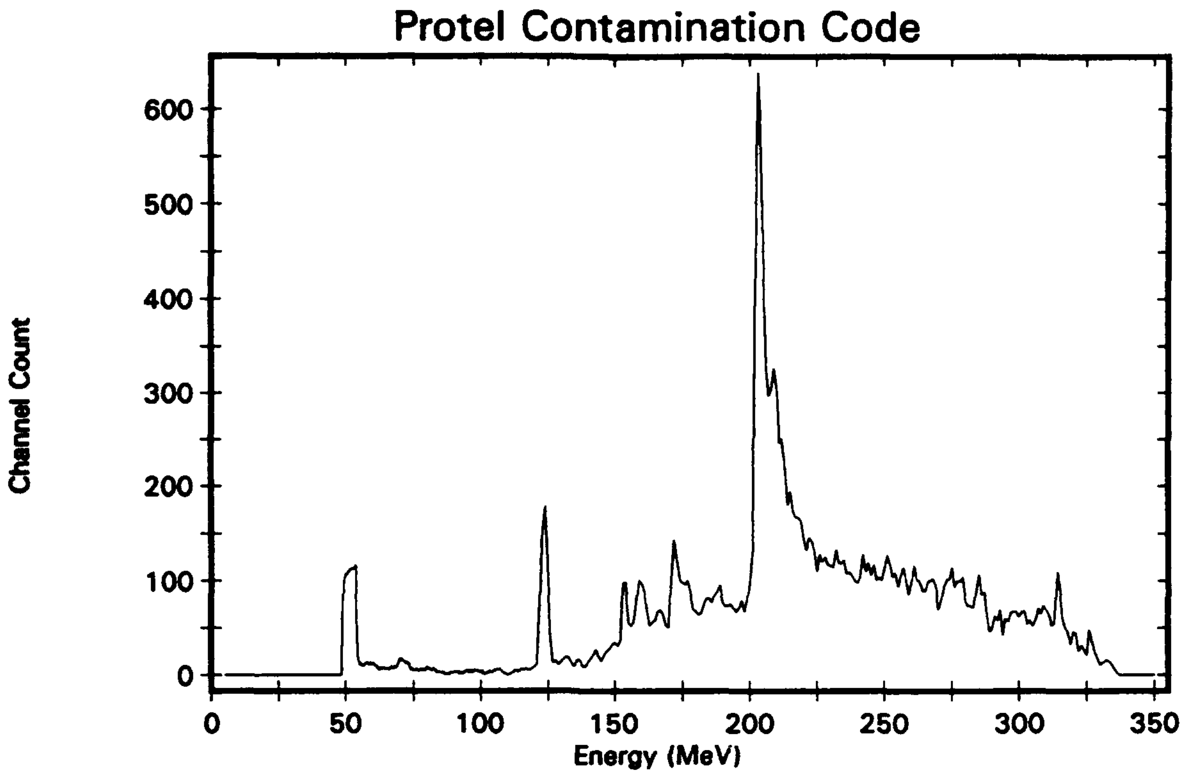

Figure B-13. Isotropic Distribution, Channel 13

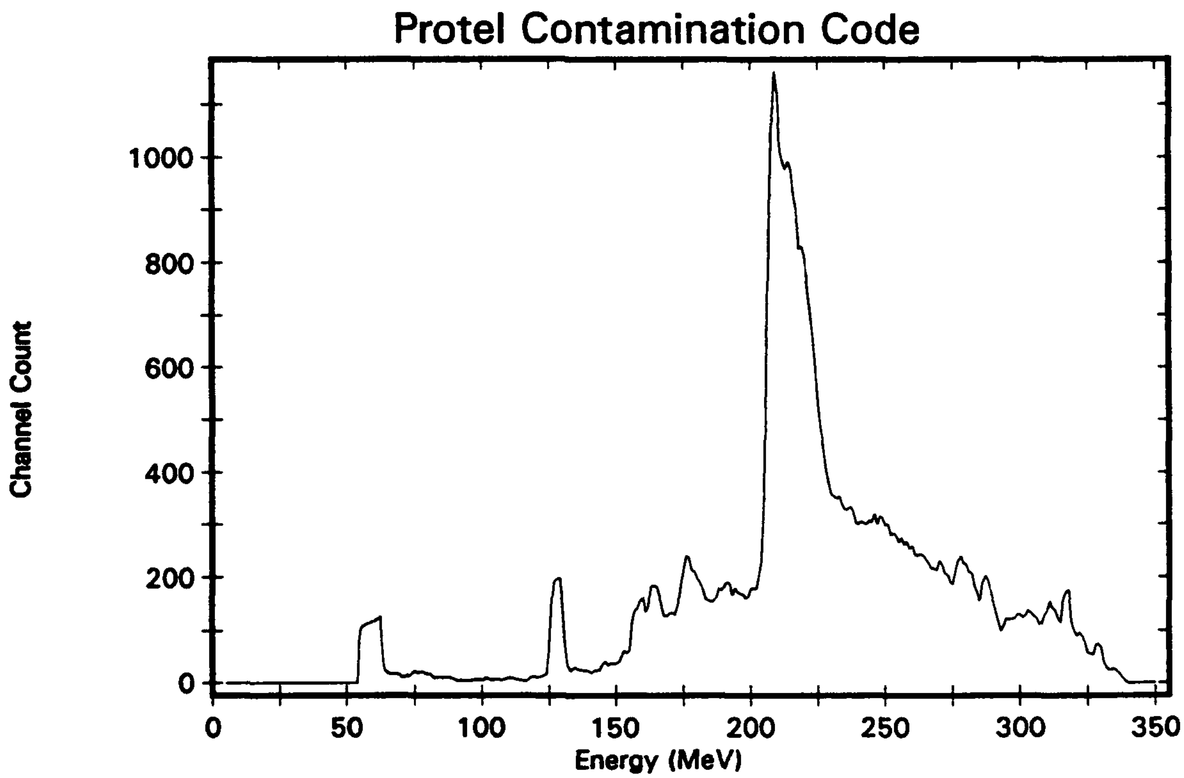

Figure B-14. Isotropic Distribution, Channel 14

DATE RUN: 8/17/93

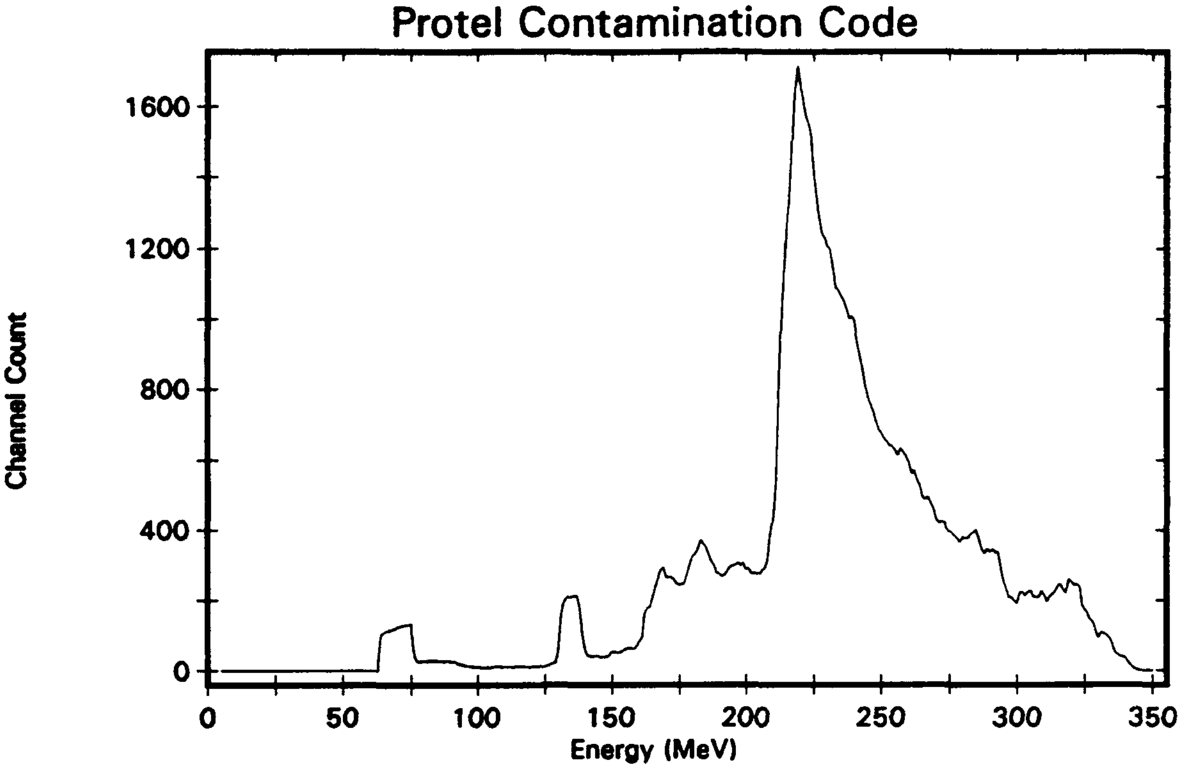

Figure B-15. Isotropic Distribution, Channel 15

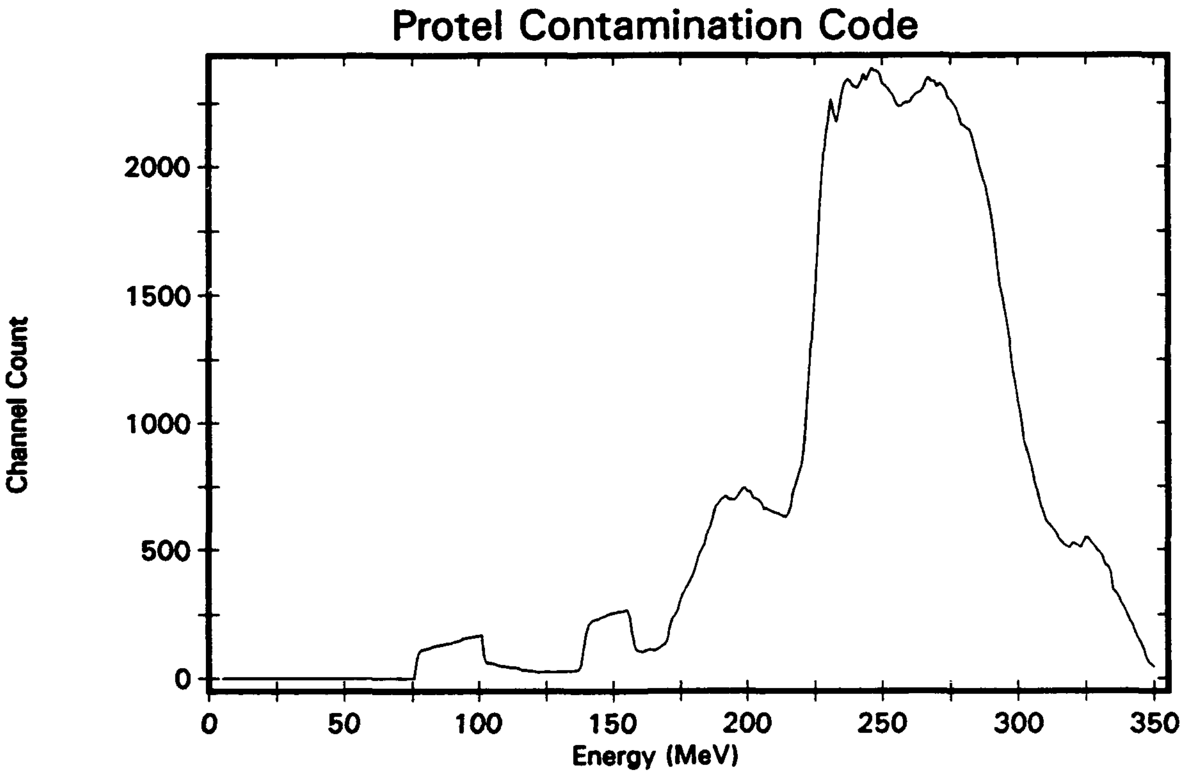

Figure B-16. Isotropic Distribution, Channel 16

DATE RUN: 8/17/93

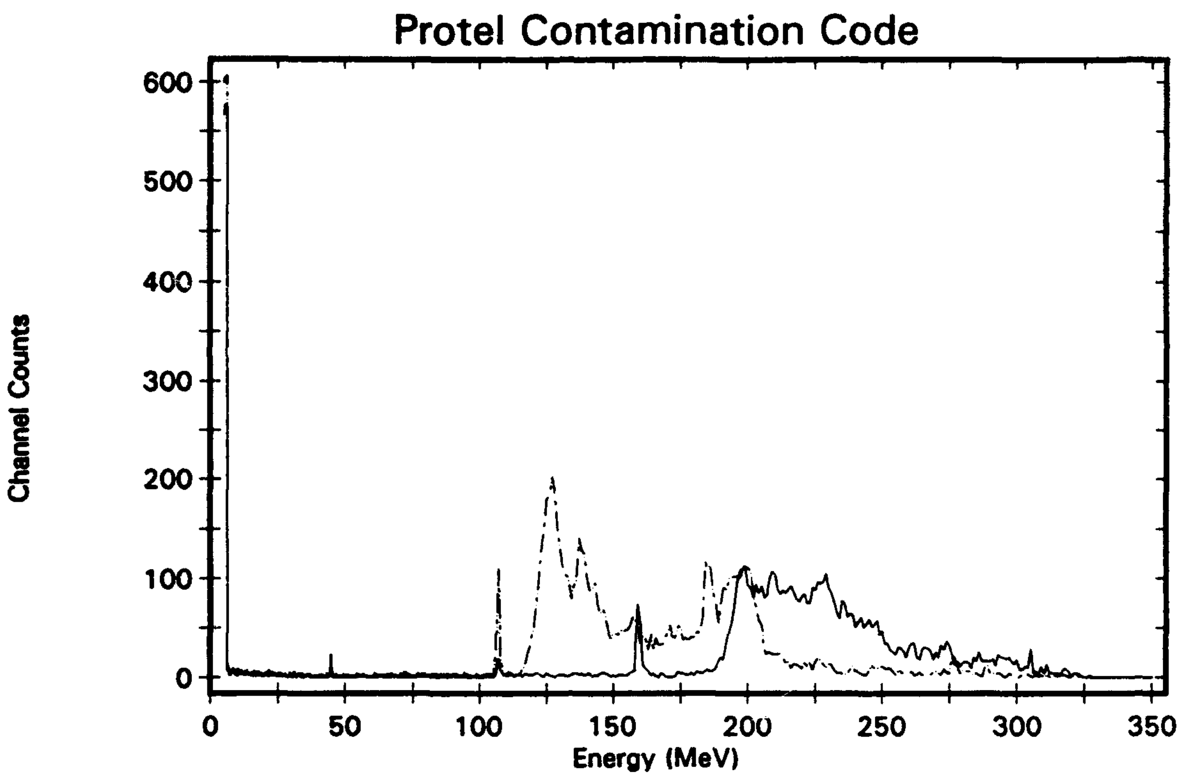

Figure B-17. Mirror Plane Distribution, Channel 1

Solid Line: 0 deg., Dashed: 90 deg. orientation with respect to Magnet

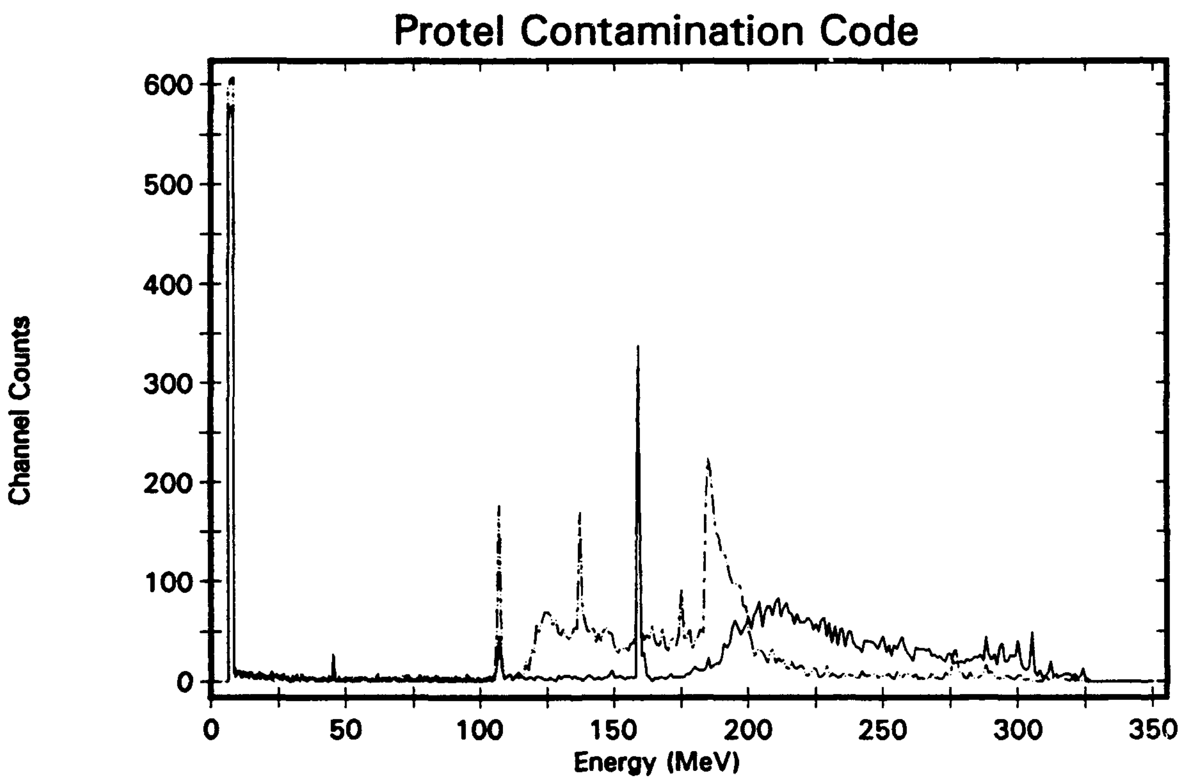

Figure B-18. Mirror Plane Distribution, Channel 2

Solid Line: 0 deg., Dashed: 90 deg. orientation with respect to Magnet

DATE RUN: 8/17/93

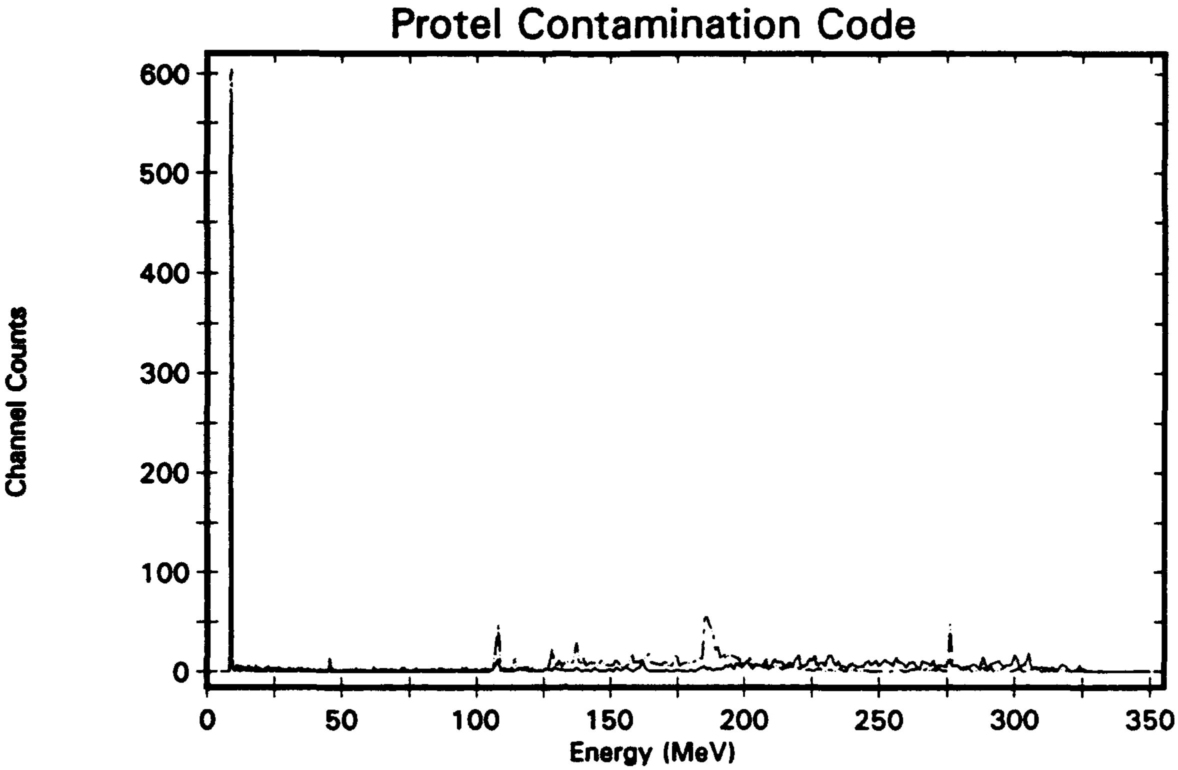

Figure B-19. Mirror Plane Distribution, Channel 3

Solid Line: 0 deg., Dashed: 90 deg. orientation with respect to Magnet

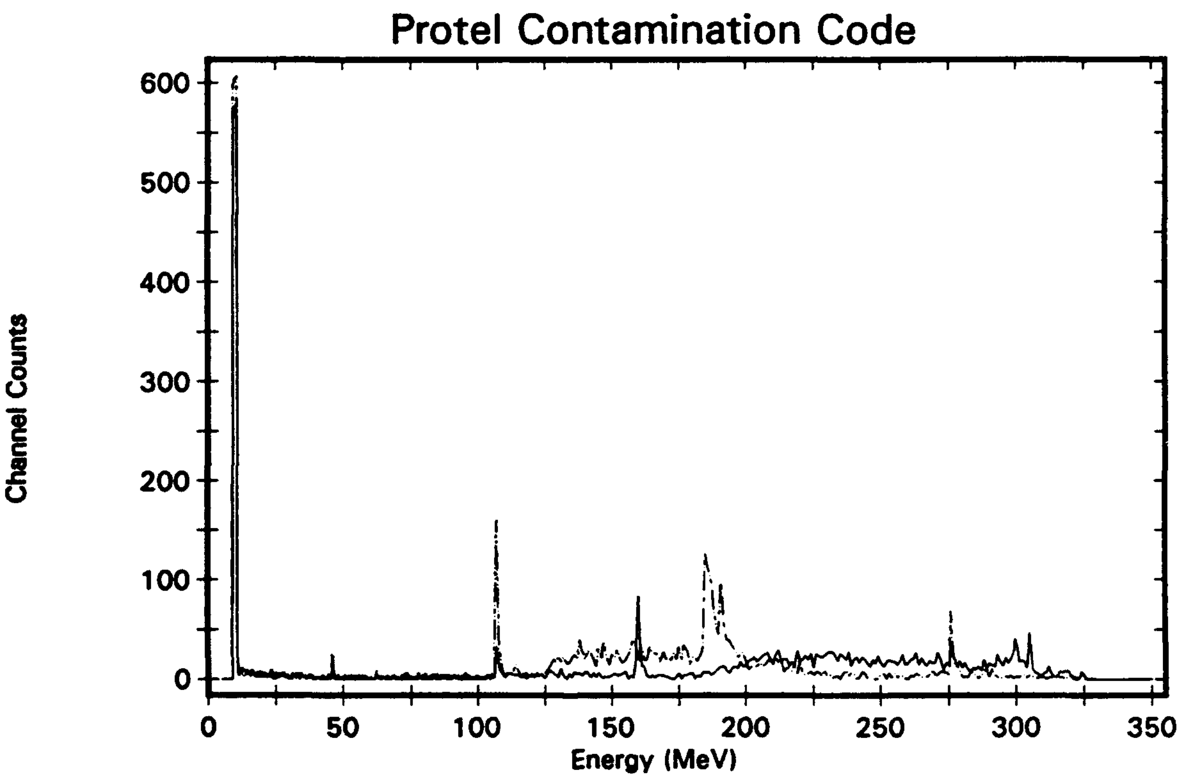

Figure B-20. Mirror Plane Distribution, Channel 4

Solid Line: 0 deg., Dashed: 90 deg. orientation with respect to Magnet

DATE RUN: 8/17/93

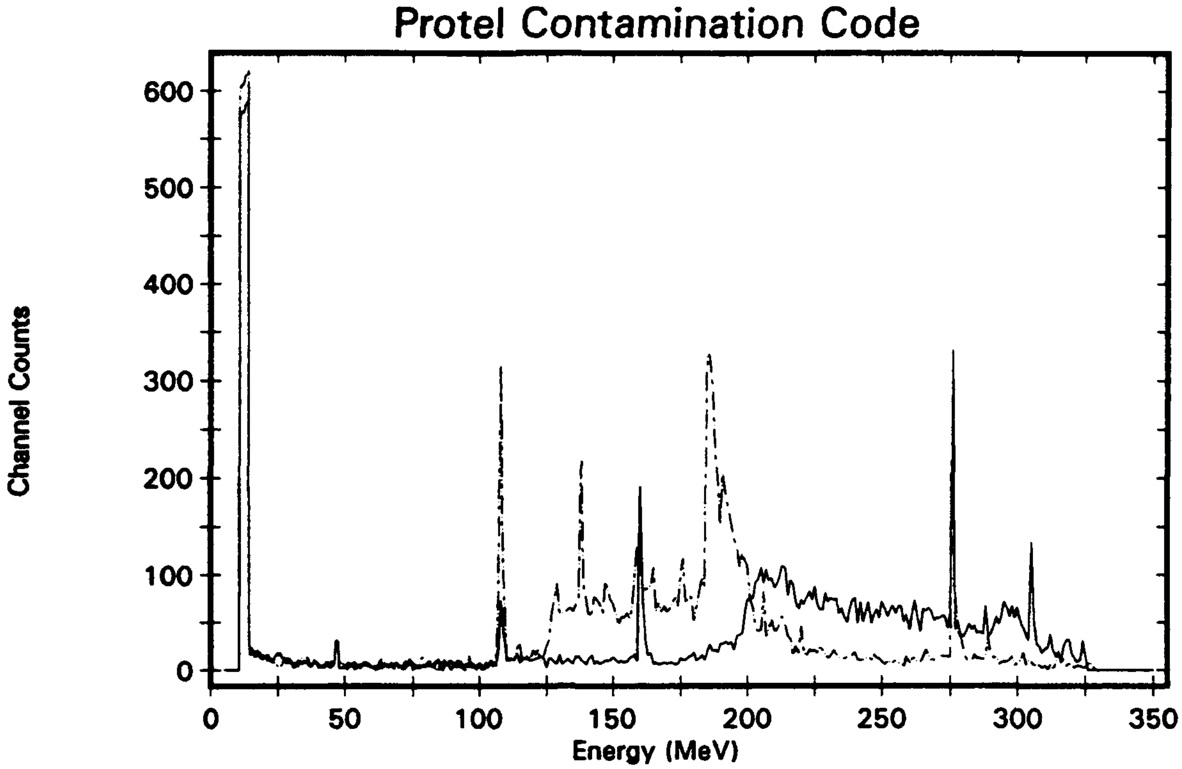

Figure B-21. Mirror Plane Distribution, Channel 5

Solid Line: 0 deg., Dashed: 90 deg. orientation with respect to Magnet

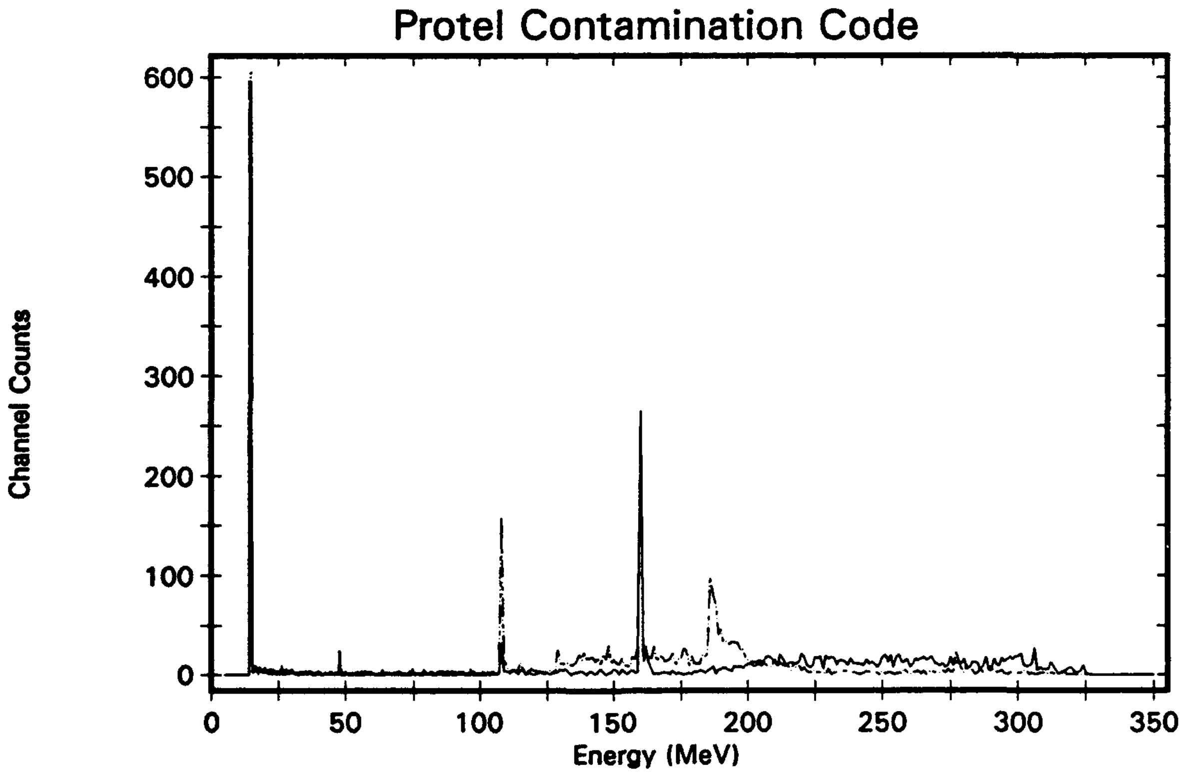

Figure B-22. Mirror Plane Distribution, Channel 6

Solid Line: 0 deg., Dashed: 90 deg. orientation with respect to Magnet

DATE RUN: 8/17/93

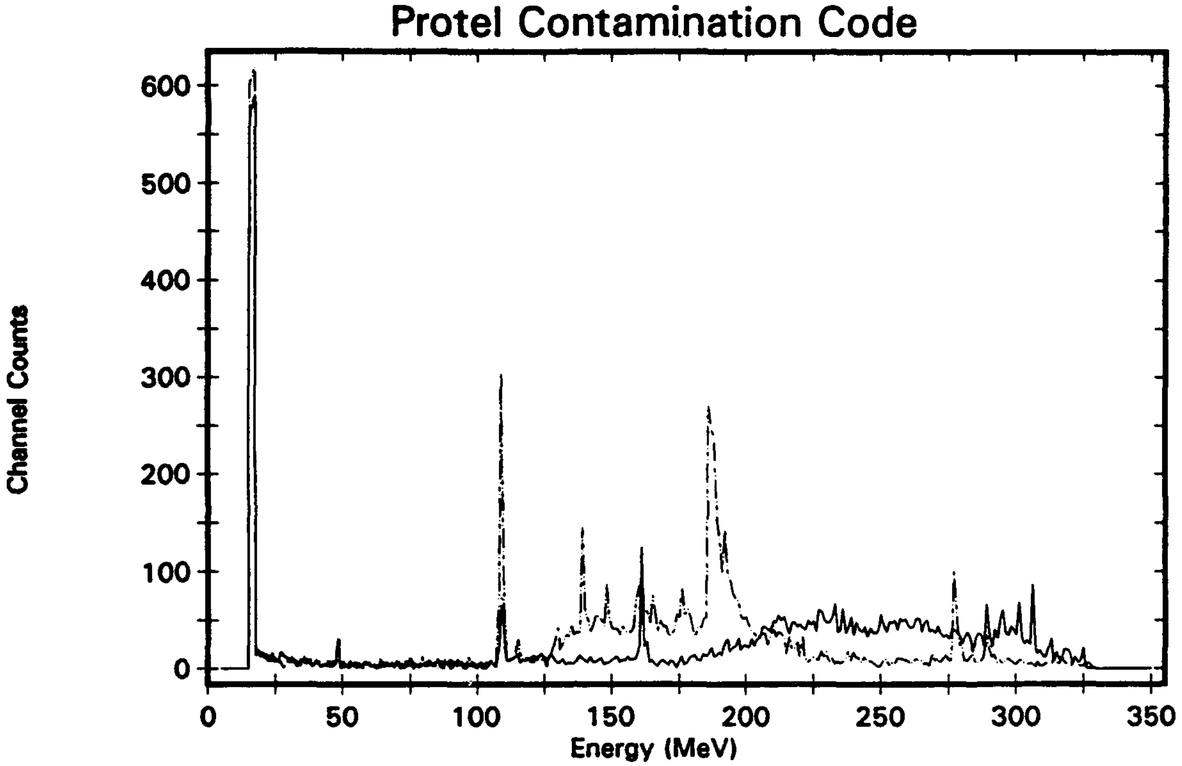

Figure B-23. Mirror Plane Distribution, Channel 7

Solid Line: 0 deg., Dashed: 90 deg. orientation with respect to Magnet

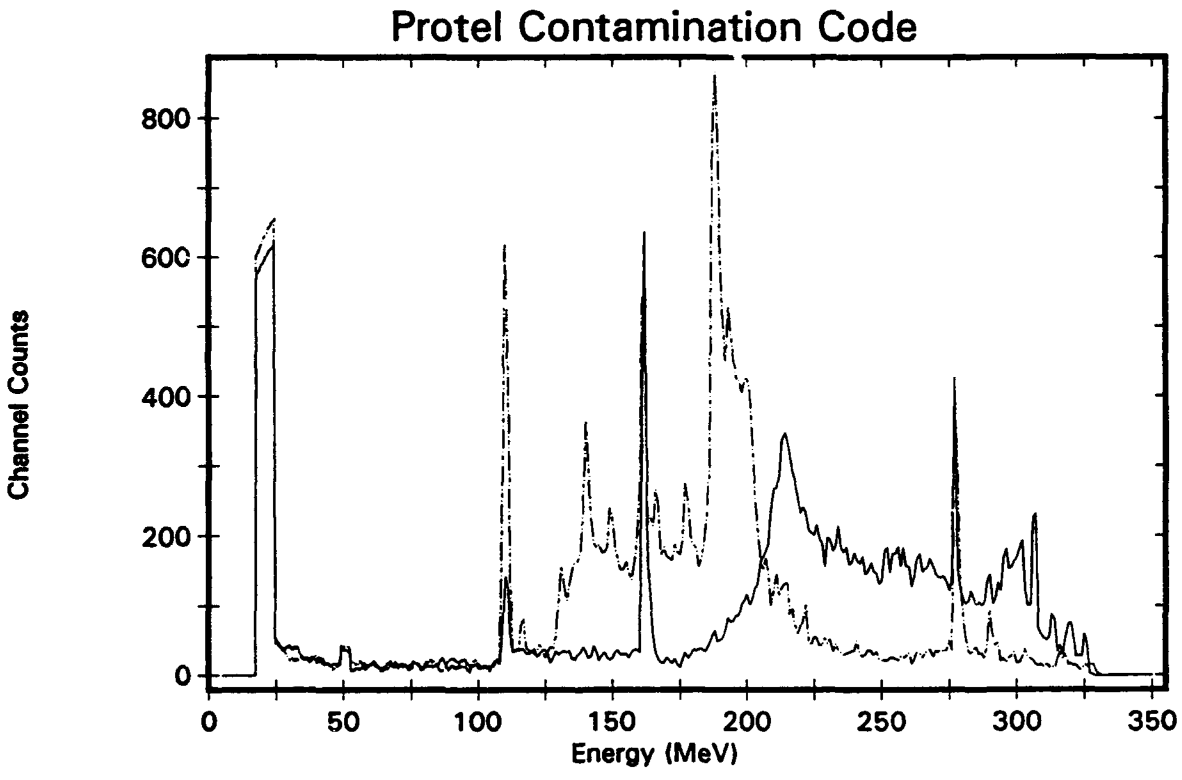

Figure B-24. Mirror Plane Distribution, Channel 8

Solid Line: 0 deg., Dashed: 90 deg. orientation with respect to Magnet

DATE RUN: 8/17/93

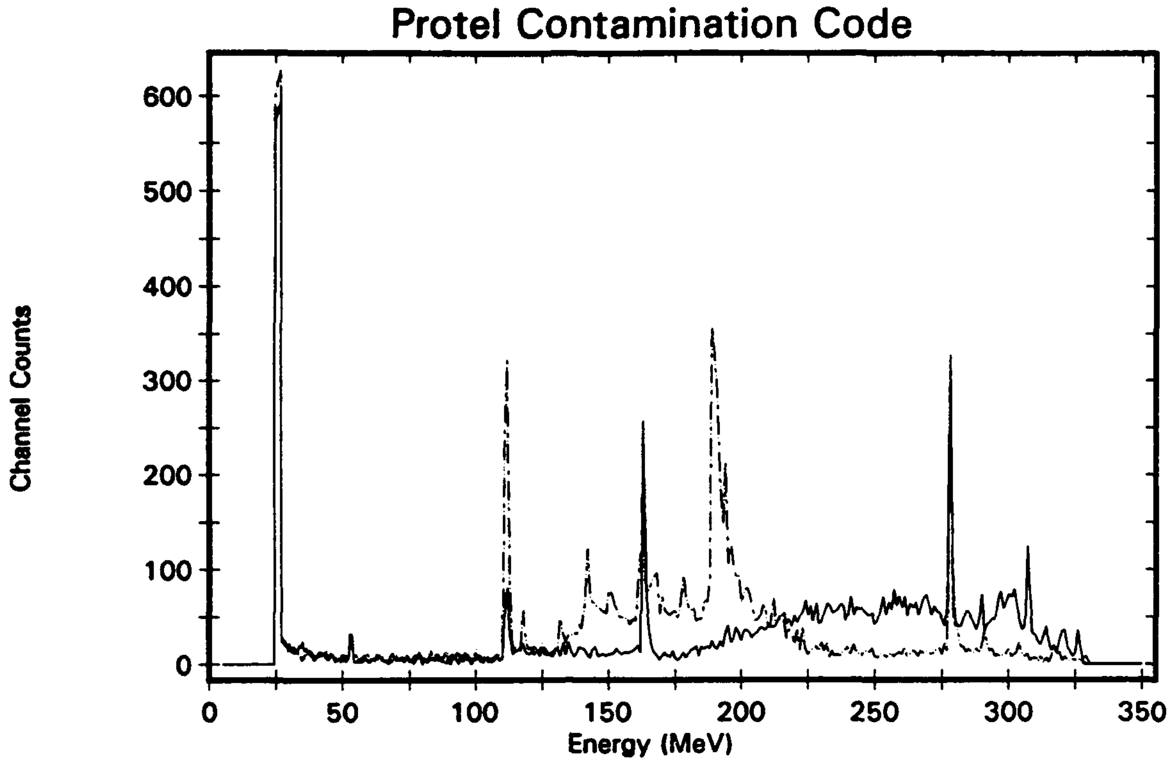

Figure B-25. Mirror Plane Distribution, Channel 9

Solid Line: 0 deg., Dashed: 90 deg. orientation with respect to Magnet

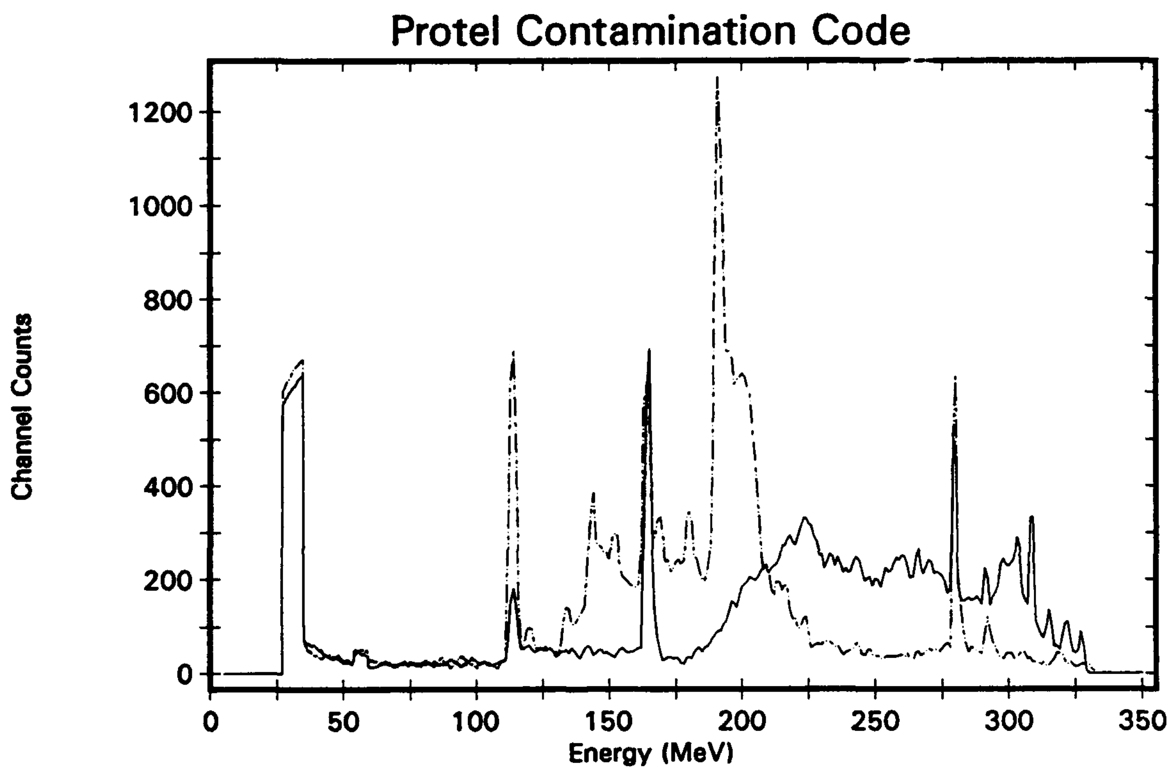

Figure B-26. Mirror Plane Distribution, Channel 10

Solid Line: 0 deg., Dashed: 90 deg. orientation with respect to Magnet

DATE RUN: 8/17/93

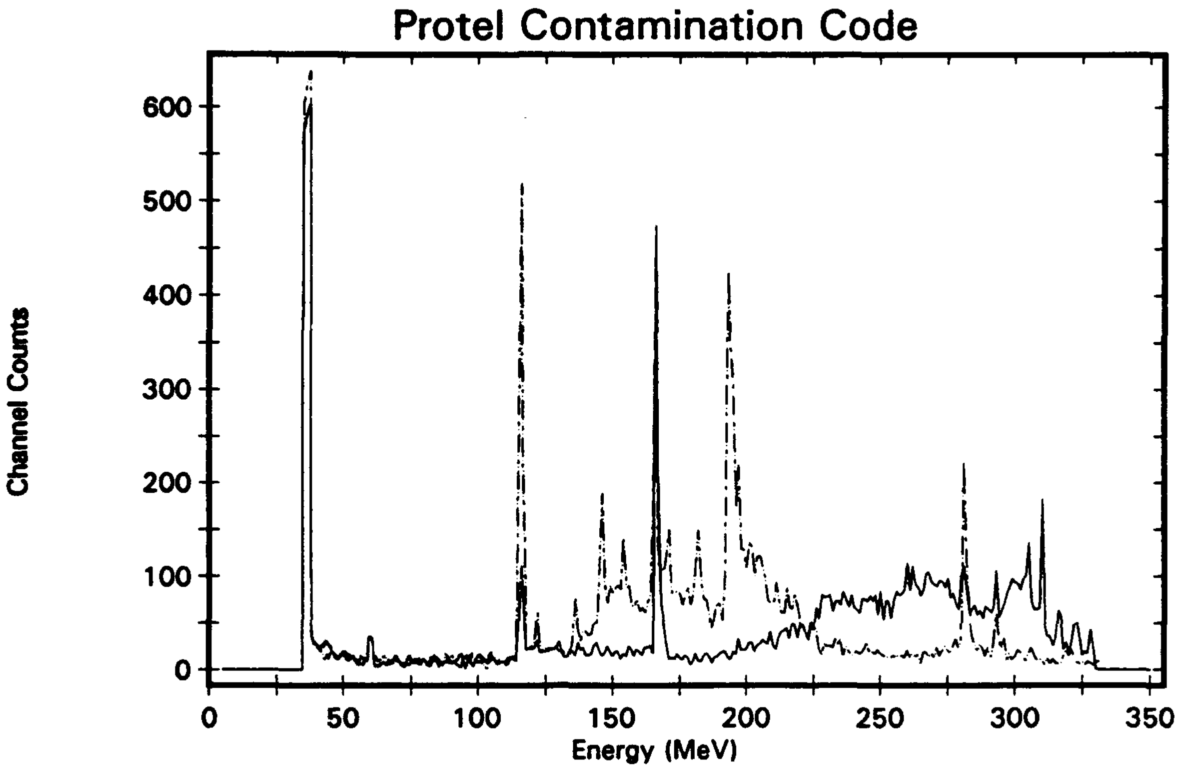

Figure B-27. Mirror Plane Distribution, Channel 11

Solid Line: 0 deg., Dashed: 90 deg. orientation with respect to Magnet

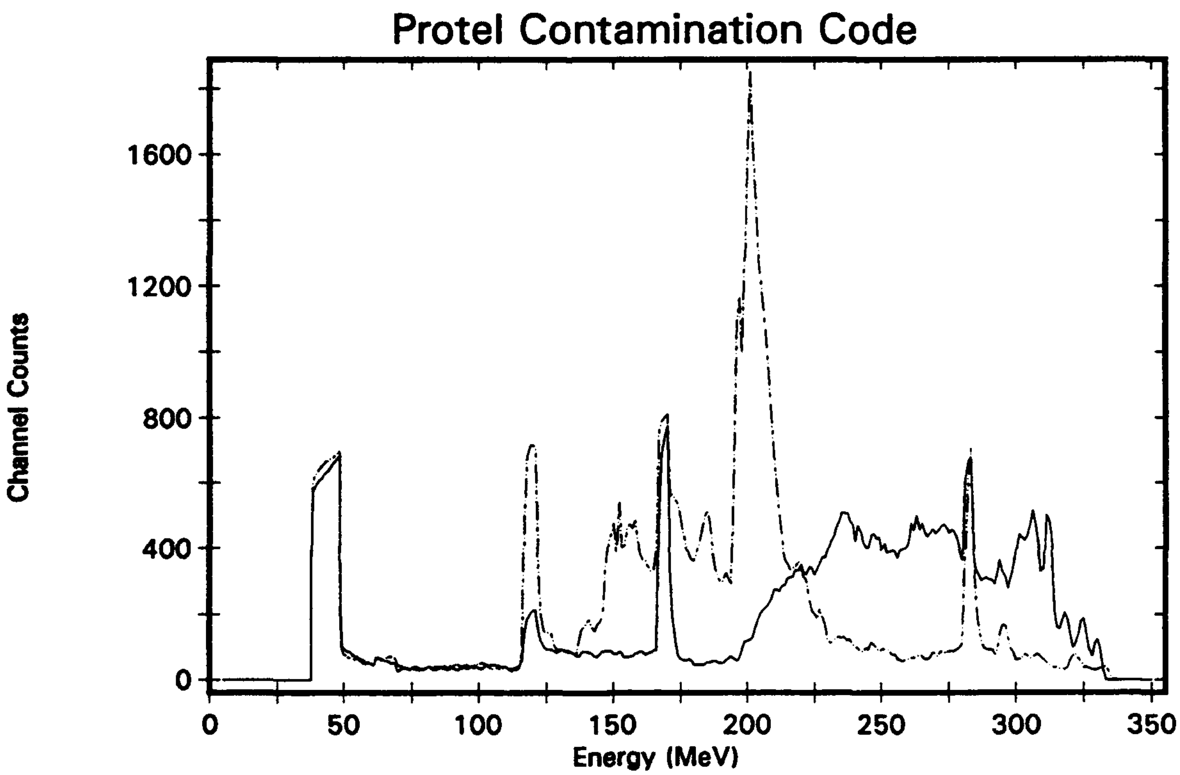

Figure B-28. Mirror Plane Distribution, Channel 12

Solid Line: 0 deg., Dashed: 90 deg. orientation with respect to Magnet

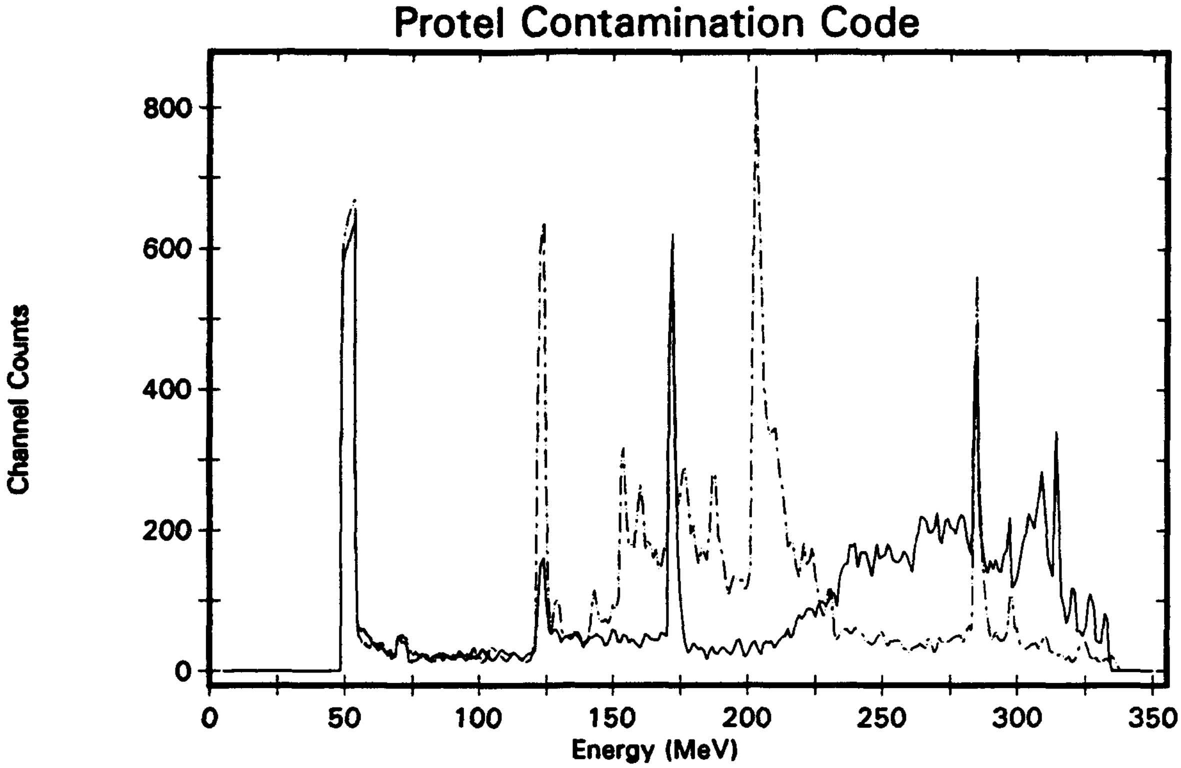

Figure B-29. Mirror Plane Distribution, Channel 13

Solid Line: 0 deg., Dashed: 90 deg. orientation with respect to Magnet

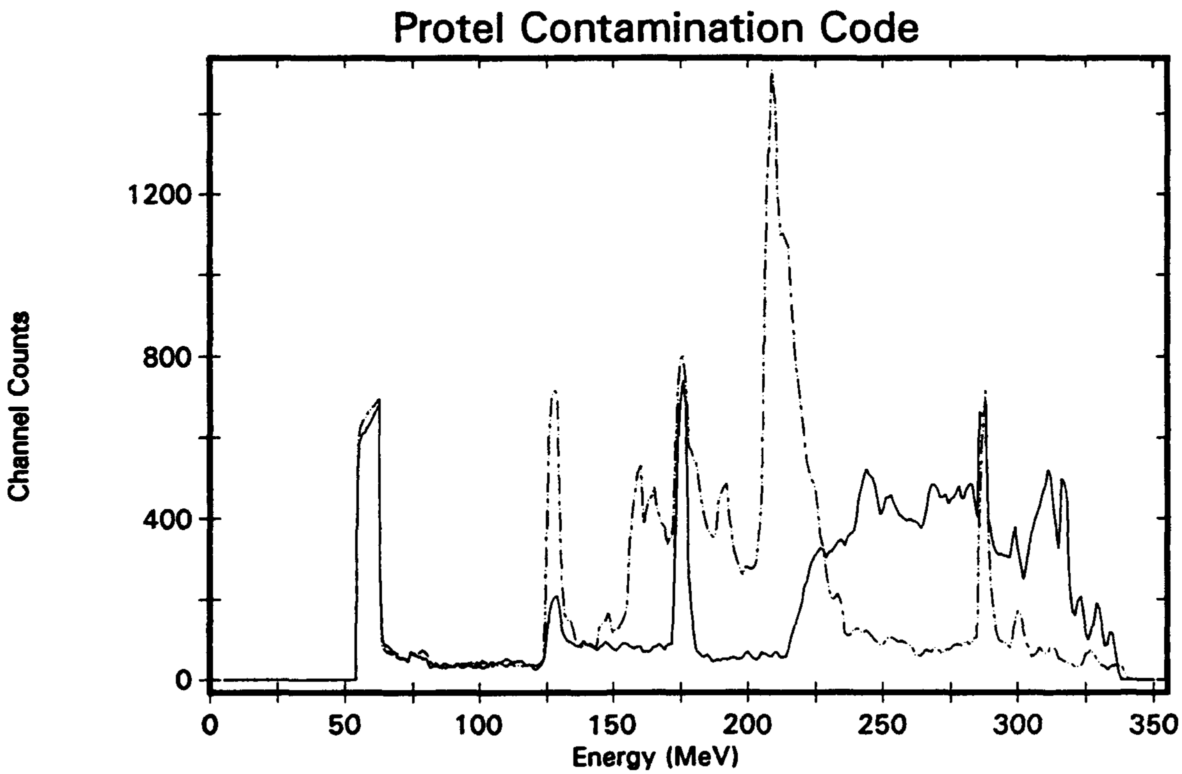

Figure B-30. Mirror Plane Distribution, Channel 14

Solid Line: 0 deg., Dashed: 90 deg. orientation with respect to Magnet

DATE RUN: 8/17/93

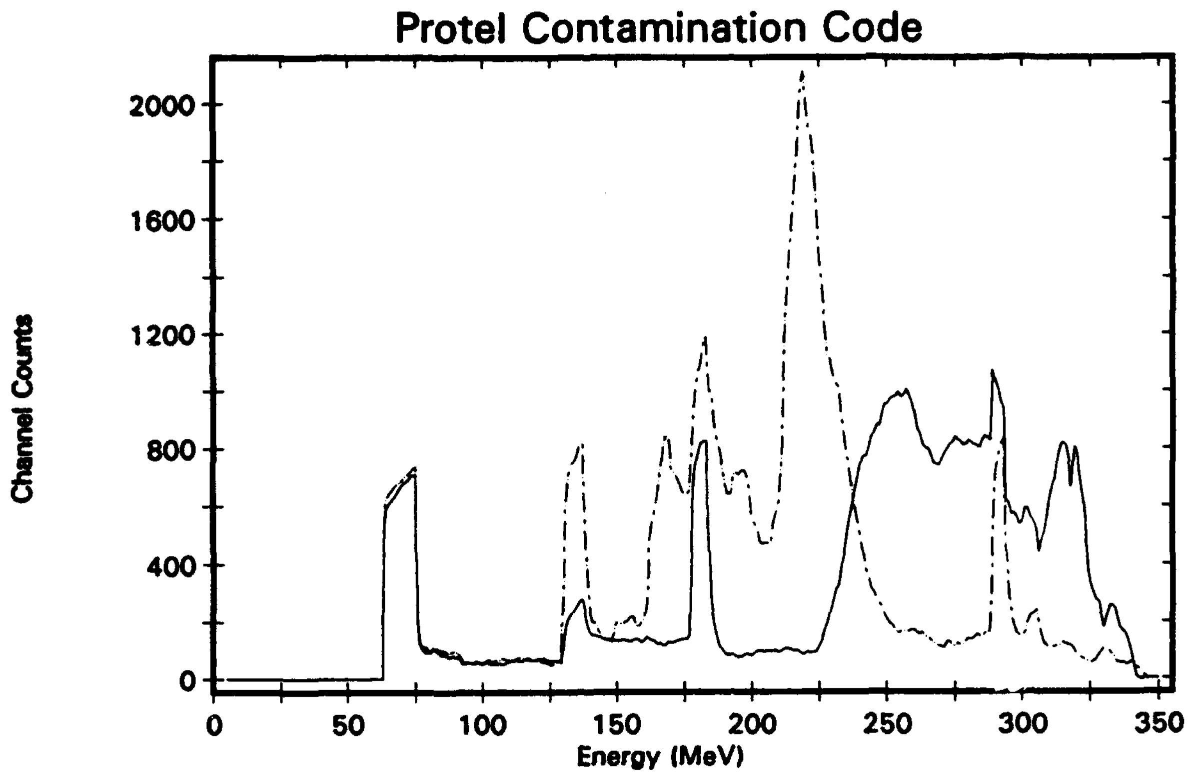

Figure B-31. Mirror Plane Distribution, Channel 15

Solid Line: 0 deg., Dashed: 90 deg. orientation with respect to Magnet

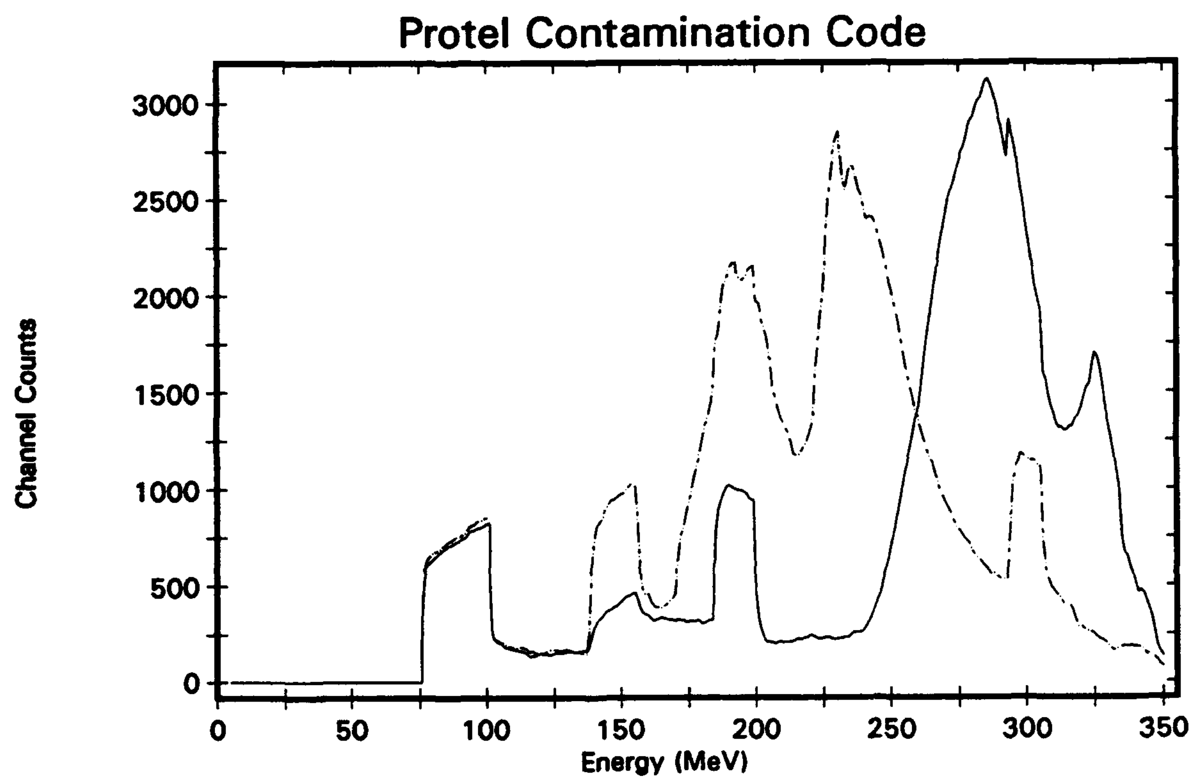

Figure B-32. Mirror Plane Distribution, Channel 16

Solid Line: 0 deg., Dashed: 90 deg. orientation with respect to Magnet

DATE RUN: 8/17/93